December 2016

In-Situ Optical Microscopic Investigation of the Dendrite Formation on Lithium Anode Under Different Electrolyte Conditions in Li-S Battery

Tianyao Ding
University of Wisconsin-Milwaukee

IN-SITU OPTICAL MICROSCOPIC INVESTIGATION OF THE DENDRITE FORMATION ON LITHIUM ANODE UNDER DIFFERENT ELECTROLYTE CONDITIONS IN LI-S BATTERY

by

Tianyao Ding

A Dissertation Submitted in

Partial Fulfillment of the

Requirements for the Degree of

Master of Science

in Engineering

at

The University of Wisconsin-Milwaukee

December 2016

ABSTRACT

IN-SITU OPTICAL MICROSCOPIC INVESTIGATION OF THE DENDRITE FORMATION ON LITHIUM ANODE UNDER DIFFERENT ELECTROLYTE CONDITIONS IN LI-S BATTERY

by

Tianyao Ding

The University of Wisconsin-Milwaukee, 2016
Under the Supervision of Professor Deyang Qu

By utilizing a high-resolution optical microscope, the dendrite formation on a lithium electrode with different electrolytes suitable for Li-S battery was investigated. It is found that the anions of lithium, the solvents, and the deposition current density have significant effects on the dendrite formation and surface morphology of lithium electrodes in electrolytes without polysulfides. On the contrary, in electrolytes with 25 mM concentration of polysulfides, the dendrite formation and surface morphology tend to be similar regardless of the other conditions. The dendrite-suppression effect of polysulfides, inorganic additive ($CsNO_3$), and electrode modifier (TEOS) are not significant in the electrolytes with polysulfides and a high deposition current density (10 $mA*cm^{-2}$).

Keywords: in-situ Optical Microscopy, lithium dendrites, lithium-sulfur battery, nonaqueous electrolyte, polysulfide

To

my family,

my colleges,

and especially Dr Deyang Qu and Dr Dong Zheng

TABLE OF CONTENTS

LIST OF FIGURES

LIST OF ABBREVIATIONS

SEM	Scanning electron microscope
SEI	Solid Electrolyte Interface
LIB	Lithium-ion batteries
EV	Electric vehicle
ID	Inside diameter
PTFE	Polytetrafluoroethylene
XPS	X-ray photoelectron spectroscopy
DME	dimethoxyethane
DOL	1,3-dioxolane
AND	1,4-Dicyanobutane
DMSO	dimethyl sulfoxide
TEOS	tetraethyl orthosilicate

ACKNOWLEDGEMENTS

Many people deserve my gratitude for helping me during my master studies. I am most thankful to my mentor and thesis advisor Prof. Deyang Qu for providing guidance and inspiration. His vast wealth of knowledge in the chemistry and batteries allows him to find solutions when my progress in an experiment is stuck. I would also like to thank Dr. Dong Zheng for providing me with training, producing the electrolyte and solvent, and answering all of my questions and giving a lot of suggestions for the experimental design.

I want to thank Professor Benjamin Church and Professor Roshan M Dsouza as my thesis defense committee members and their suggestions to my thesis and future work.

I also want to thank the Johnson Controls for their generous funding for the lab equipment. Without these machines especially the glove box, it's impossible to make a lithium cell. I also want to thank the members of my research group that I worked with, Josh Harris, Dan Liu, Gongwei Wang, Jingyu Si and Sergei Andrew for their time and support in helping me become familiar with the equipment in the lab.

I would thank my family for their love and support of my studies.

This work was supported by the Assistant Secretary for Energy Efficiency and Renewable Energy, Office of Vehicle Technologies, under the program of Vehicle Technology Program, under Contract Number DE-SC0012704. The authors from WUT are grateful for the support from Fundamental Research Funds for the Central Universities (WUT: 2015-IB-001)

1. Introduction

Recently, rechargeable lithium sulfur (Li-S) batteries have drawn significant attention due to their high theoretical energy density, 1675mAh g^{-1}, which allow it to be considered as a potential candidate to replace the state of-art Lithium-ion batteries (LIBs) that are currently found in electric vehicles (EVs). Although the rechargeable Li-S battery has been investigated over three decades, many critical issues remain to be addressed, such as low rechargeability and high self-discharge rate compared to the commercialized LIBs. In order to utilize the extremely high energy density of Li-Air and Li-S batteries, a Lithium metal anode instead of lithium insertion anode as in traditional LIBs must be used. Although lithium metal is very chemically reactive, the lithium metal anode in Li-Air or Li-S batteries are actually safe at the research scale due to the passivation of the surface of the lithium metal by the electrolytes and other chemicals. The biggest issue for the lithium metal anode in rechargeable Li-Air and Li-S batteries is the formation of lithium dendrites on the anode surface during charging due to lithium deposition. [1] The penetration of dendrites through the separator will cause an electrical short in the battery, thus the inhibition of dendrite growth is of great importance for any kind of rechargeable lithium battery with a lithium metal anode (i.e. Li-Air and Li-S batteries). [2]

Although the mechanism for lithium dendrite formation is still not clear, the complexity of the lithium dendrite formation has been greatly recognized and demonstrated. Lots of factors influence the dendrite formation on lithium anode, such as solvents, lithium salts, concentration, temperature, current density, and additives.[3-31] It's widely accepted that the solid-electrolyte interphase (SEI) layer formed on the lithium surface is a key factor for the formation of lithium dendrites.[1,2] Anything that could influence the chemical and physical properties of the SEI layer may potentially influence the formation of lithium dendrites during the lithium deposition

process. In a Li-S battery, the discharge products of the sulfur cathode, lithium polysulfide species, are soluble in an ether-based electrolyte, and thus potentially those lithium polysulfide species could influence the lithium deposition process on the lithium anode during charging. In recent work, Mikhaylik *et al* reported imaging with SEM a mossy/powder like surface was developed on the lithium anode in a Li-S battery due to the shuttle effect between polysulfide species and lithium the anode [17]; Cui *et al* reported that there is a synergetic effect of lithium polysulfide in preventing lithium dendrite growth by SEM and *in-situ* optical microscopy [32]. To further investigate the influence of polysulfide species on the lithium dendrite formation in Li-S battery an optical microscope was used in this work to in-situ monitor the lithium deposition and stripping in a modified electrochemical cell with electrolyte conditions mimicking those in a real Li-S battery.

To introduce the reader to the topic, a brief introduction of the background knowledge will be presented, which includes the introduction of a Li-S battery and dendrites. The main part of the thesis will discuss how the dendrite growth process differs in different electrolyte environments and compare the results to determine the effect that different electrolytes and additives will have on dendrite growth. Last this thesis ends with a short conclusion and the future work.

1.1 Brief introduction about lithium sulfur batteries.

The first concept of Lithium-sulfur batteries was introduced in the early 1960s [51], which used lithium as the cathode and sulfur as anode. Although it has been investigated for more than 50 years lithium sulfur batteries still suffer from low rechargeability and high self-discharge rate when compared with other Lithium batteries. In the year of 2009, Nazar [52] developed a Polyethylene glycol coated, pitted mesoporous carbon cathode. The conductive mesoporous carbon framework encapsulate sulfur within its channels. This structure made a breakthrough for the capacity and cycling stability of the Li-S battery. Since then, more and more researchers are focusing on this field and a lot of papers have been published on this topic.

The Lithium-sulfur battery is a promising energy storage system because of its high energy density compared to existing lithium-ion batteries. The main difference is the way that the lithium sulfur batteries store energy. It operates based on metal plating and stripping on the lithium anode side and a conversion reaction on the sulfur cathode side. The reaction of lithium with sulfur could perform a 2 electron transfer which means the sulfur could deliver a theoretical specific capacity of 1675 mAh/g. The lithium electrode theoretically capacity is 3860 mAh/g. [53] The calculated theoretically energy density of the lithium sulfur battery is 2600Wh/kg, which is much higher than most lithium batteries. If the battery's real energy density could achieve 20% of the theoretical value, the battery would make a revolution in the battery market with its 500Wh/kg energy density. This is the reason that the lithium sulfur battery is one of the hot topics in high energy capacity battery research. Also sulfur is one of the most abundant elements on the earth so it will help the manufacturer lower the cost of the lithium battery; also sulfur is an environmental-friendly element (i.e. no hazardous waste generated).

But lithium sulfur battery still needs to overcome some problems. First is the high resistance of sulfur. Sulfur's conductivity at room temperature is $1.0*10^{-15}$S/m, which is very low. Also the final products for the reaction Li_2S_2/Li_2S are all electrical insulators, which will affect the working efficiency of the battery. Second, the polysulfide ion can migrate between the cathode and anode. The increase in this ion will increase the electrolyte's viscosity and lower the conductivity; this is called the "shuttle effect". Third, the product Li_2S_2/Li_2S may not dissolve in the electrolyte and may be deposited on the conductive frame which will drastically lower the capacity. Fourth, the massive difference in the structure of sulfur and lithium sulfide will result in a large volume expansion and contraction when charging and discharging. Those volume changes will change the structure of the electrode and lead to the sulfur separating from the conductive frame hence causing capacity loss and damage to the battery. This swelling effect becomes more dangerous when applied on batteries of larger volume. Last, the lithium electrode will also have a volume change when the battery is at charge versus discharge state. Also dendrites will grow on the surface of the lithium electrode and could cause safety issues. These issues are the reason why the lithium sulfur battery has yet to be commercialized.

1.2 Brief introduction about dendrite formation

Dendrite growth during battery charging has been identified as one of the critical issues for the safety of batteries. Dendrite growth not only happens in lithium metal but other metals such as Zn, Cu, Ag etc. They are reported to exhibit branched morphologies. [1] The fractal growth pattern contains many shapes. The needle-like growth will be called one-dimensional growth. The tree-like, bush-like and moss-like growth will be counted as three dimensional growth.

Dendrite growth has also been identified as an important factor in performance degradation. If the dendrite falls off from the deposition surface, it will cause a loss of capacity. Separate of that, if the dendrite keeps growing, it will penetrate the separator of the battery which has a thickness around 20 to 30 micrometers. After it penetrate the separator, it will keep growing and let the cathode attach to anode and cause an electrical short. The short will generate a lot of heat which will lead to problems like fires and explosions.

The contributing factors to dendrite growth are still under debate, but the current accepted theory is that the largest contributors are the solvents, salts in the electrolyte, additives and other treatments. In this thesis we will compare dendrite growth under different conditions (varying the components mentioned above) to better understand the dominating factors of dendrite growth.

2. Experiment

2.1 Chemicals.

The chemicals we used in this experiment for the electrodes and electrolytes are: Sulfur (99.98%), lithium metal (ribbon, 0.75x19 mm, 99.9%), lithium nitrate ($LiNO_3$, 99.99%), lithium sulfide (Li_2S, 99.98%), cesium nitrate ($CsNO_3$, 99.999%), tetraethyl orthosilicate (TEOS, 99.999%) (from Sigma Aldrich), dimethoxyethane (DME), 1,3-dioxolane (DOL), lithium perchlorate ($LiClO_4$), lithium difluoro(oxalate) borate (LiDFOB), lithium trifluoromethanesulfonate (LiTFS) (battery grade from FERRO), lithium bis(trifluoromethane) sulfonimide (LiTFSi), lithium-bis(oxalate)borate (LiBOB), 1,4-Dicyanobutane (ADN), dimethyl sulfoxide (DMSO), cobalt(II) phthalocyanine, lithium bis(perfluoroethylsulfonylimide) (LiBETFSi) (battery grade from 3M) were purchased and used without further treatment. The structure of some salts and organic solvents are presented in the figure 1.

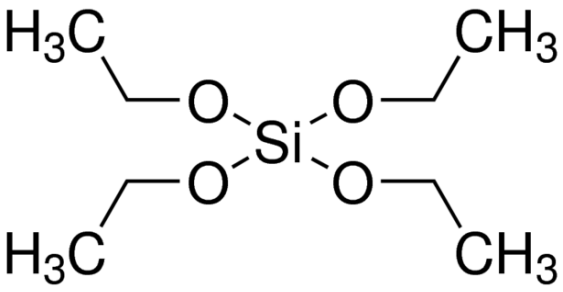

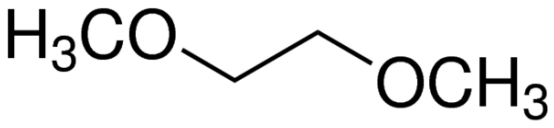

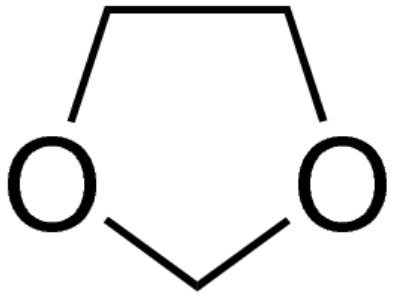

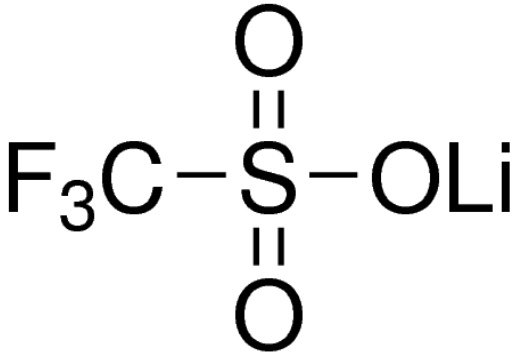

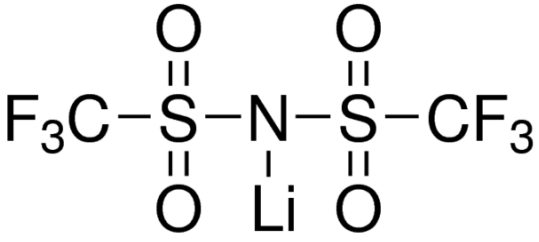

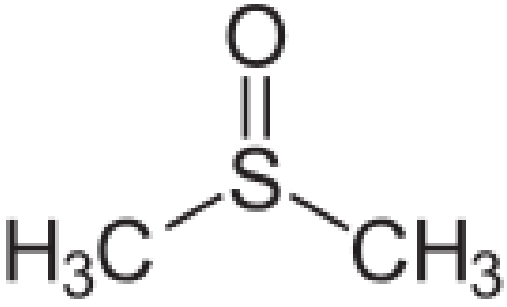

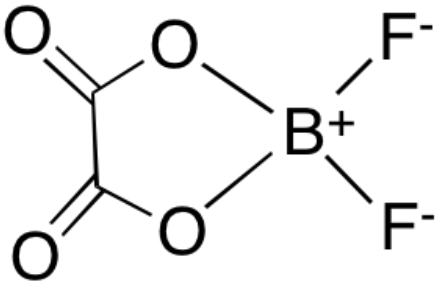

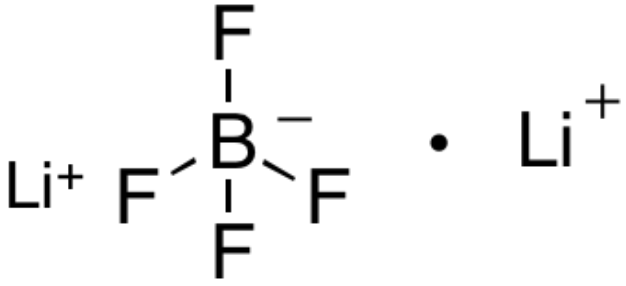

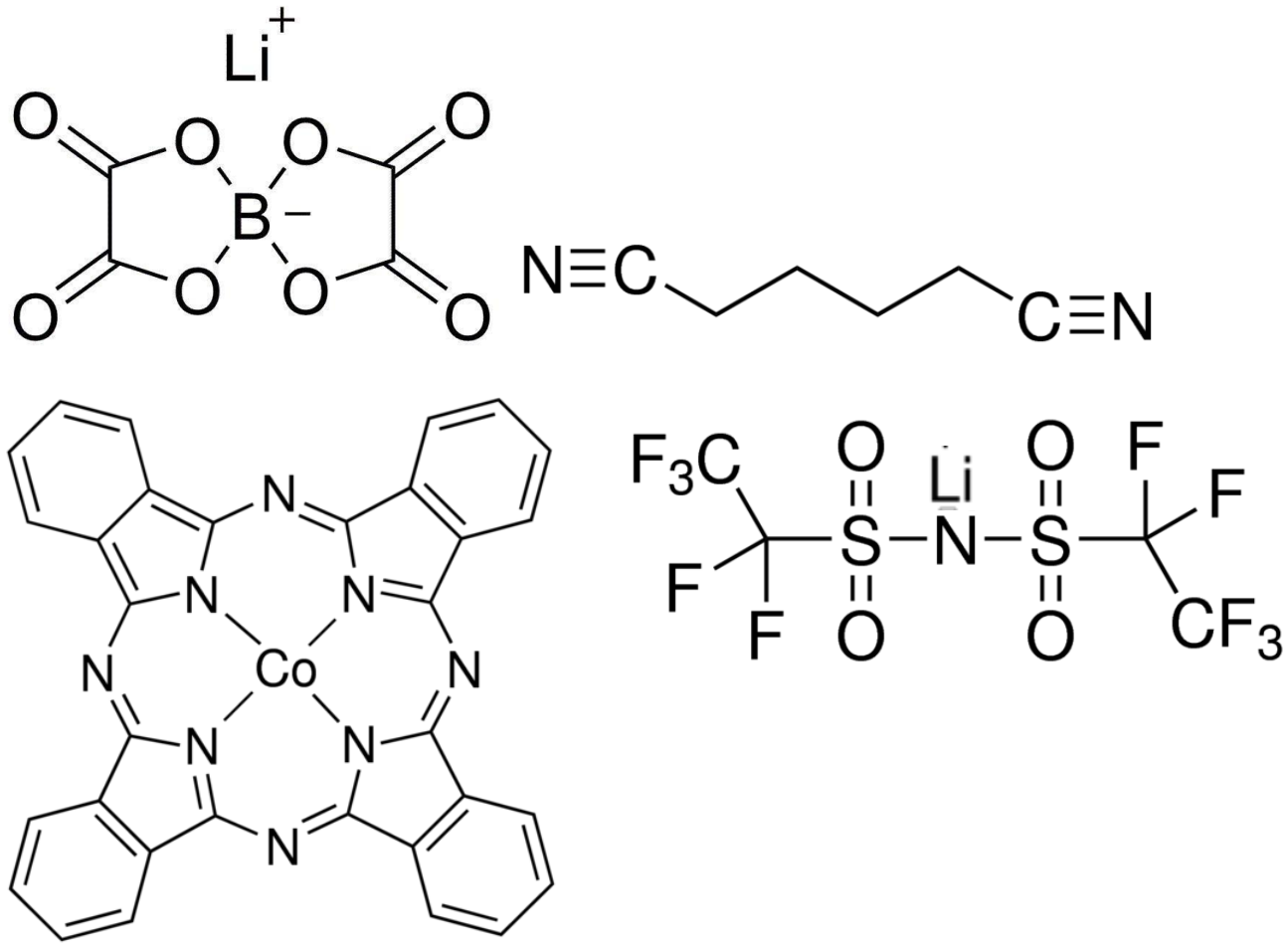

Figure 1. Structures of the electrolyte salt and organic solvent which was used in the experiment.

From left to right, top to bottom is: (1) TEOS (2) DME (top right) (3) DOL (4) LiTFS (5) LITFSI (6) DMSO (7) LIDFOB (8) LIBF4 (9) LIBOB (10) ADN (11) Co (II) phthalocyanine (12) LIBETFSI

2.2 Sample preparation and method

All baseline electrolytes were made in DME/DOL (1:1, vol) mixture, with 0.1 M $LiNO_3$, and 1 M lithium salts. All electrolytes with polysulfide species were obtained by mixing S_8 and Li_2S (molar ratio of 5:8, to form Li_2S_6 stoichiometrically) to reach a final concentration of 25 mM.[33]

The self-made air-tight cell used in this work was shown in figure 1. In general, a lithium disk (roughyl 5 mm ID and 5mm thickness) was pressed on the bottom current collector (as shown in figure 1) as the working electrode; and a lithium ribbon (with 0.75mm thickness) was pressed on the side current collector (as shown in figure 1) to form a lithium ring electrode as the reference/counter electrode; the working distance between two electrodes is about 2 mm. A glass disk (from Edmund Optics) with 40mm ID and 0.635 mm thickness was used as the observation window for optical microscope. The lithium working electrode surface was polished with a knife to obtain a shiny surface. The cell was assembled in Argon-filled glove-box with 1.0 ml of the different electrolytes mentioned above. For the silicate coated lithium electrode, 100 ul of TEOS was added onto the polished lithium working electrode and after 5 min the TEOS was removed by a micro-pipette. [34]

A Keyenece VHX-2000 optical microscope was used to observe the dendrite formation on the lithium disk of the working electrode in the two-electrode cell. During observation, the cell was operated under galvanostatic condition as follows: lithium deposition current on working electrode (lithium disk) is set at 2 mA (current density is 10 $mA*cm^{-2}$) for one hour, unless specified by other conditions. A BioLogic electrochemcial station (from BioLogic Science Instruments) was used for the galvanostatic lithium deposition experiments.

All the pictures in this thesis were taken by the digital camera that is installed on the microscope. There are two methods of recording images with the Keyence. The first method is depth composition method. This mode is used to digital 3D image something. In this mode the cell is placed on the microscopes x-y stage, which remains fixed the entire time. The camera above the x-y stage moves along the z axis taking pictures in increments of 10 micrometers. Upon completion the software finds the best resolution for each part and stacks all the picture together to form a new in-focus 3D depth profile of the images. The second mode of photography is called stitching. In this mode the cell is placed in the center of the microscope's X-Y stage. The x-y stage will then move in the x-y plane in a clockwise fashion around the center point. It will stop for each position to finish the depth composition process, then move to another position and repeat the steps. Upon completion the software stitches all the images together forming one larger picture which is used as the figure in the later part of the thesis. Last, the deposition of the lithium dendrite is recorded in-situ by the video camera on the microscope for every experiment.

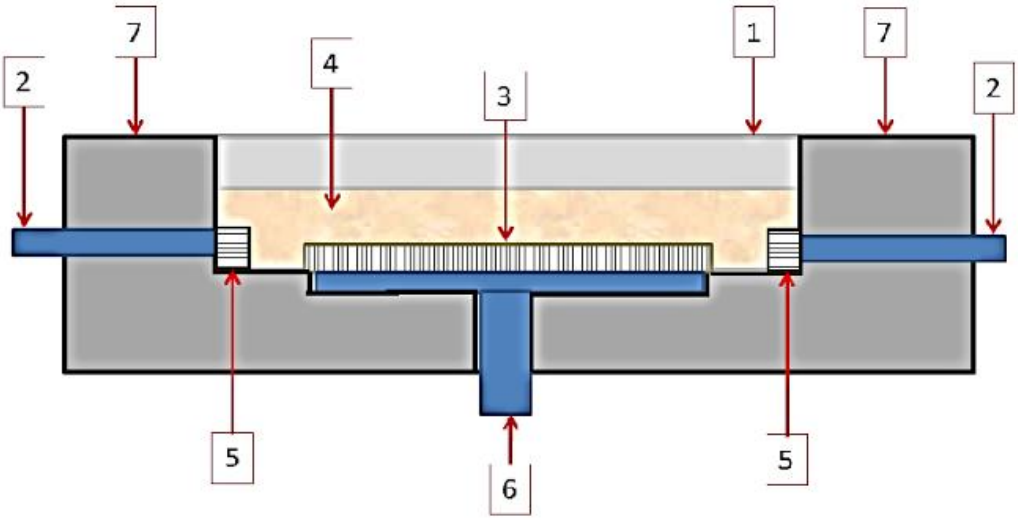

Figure 2. Schematic set-up of the self-made two-electrode cell in this work.

1, observation glass window; 2, steel current collector for reference/counter electrode; 3, lithium disk of working electrode; 4, electrolyte; 5, lithium metal of reference/counter electrode; 6, steel current collector for working electrode; 7, PTFE body of the cell.

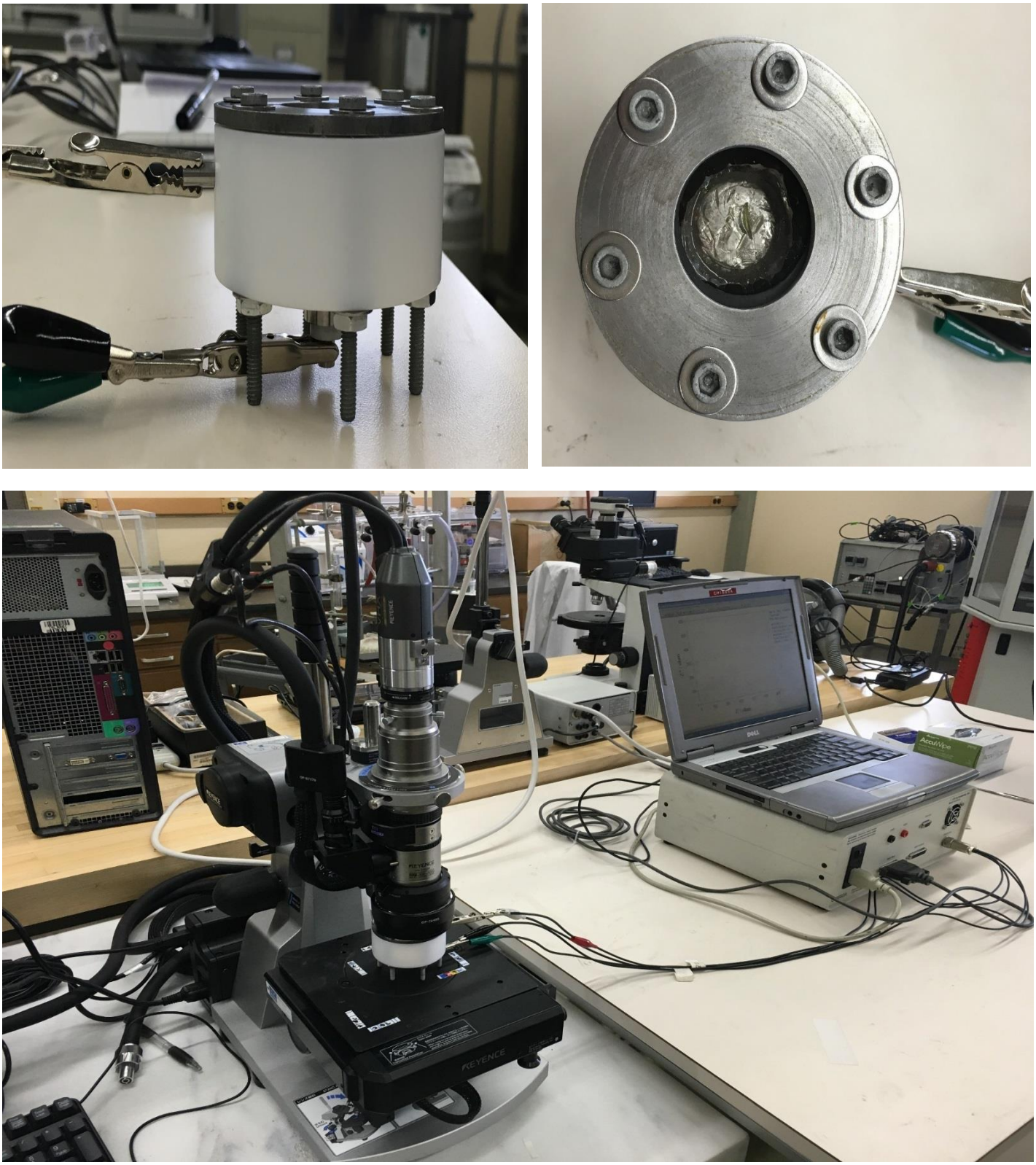

Figure 3 Experiment setup and cell's side view and top view

3. Result and discussion

3.1 Lithium dendrite morphology in electrolytes without lithium polysulfide.

Typically, most of Li-S batteries are tested in the ether-based electrolytes, and the most popular electrolytes are the LiTFSi in DME and DOL mixture with 0.1 M to 0.3 M $LiNO_3$ (as a polysulfide shuttle inhibitor). [33, 35-37] Other suitable lithium salts include LiTFS and $LiClO_4$.[36,37] Due to the similar molecular structure of LiBETFSi to LiTFSi and the relative stability of LiDFOB with polysulfide [33], LiBETFSi and LiDFOB were also included in this study. A total of 5 lithium salts in DME/DOL without polysulfide species were first investigated due to their suitability for a Li-S battery. Figure 4 shows the morphologies of the whole lithium electrodes before and after lithium deposition in electrolytes with different lithium salts. Clearly at that high deposition current density (about 10 $mA*cm^{-2}$) dendrites with different morphologies are formed on the lithium surface of the electrodes. Due to the setup of electrochemical cell (disk and ring electrodes), most of the big dendrites are formed in the outer part of the lithium disk electrode, but only limited and small dendrites are formed in the center of electrode. Relatively the deposition in electrolyte with 1 M LiDFOB salt has bigger dendrites in size compared to the dispositions in electrolytes with other lithium salts, as shown in figure 4(C) (indicated in blue oval) there are multiple sites that the dendrites almost reach the ring electrode (counter electrode).

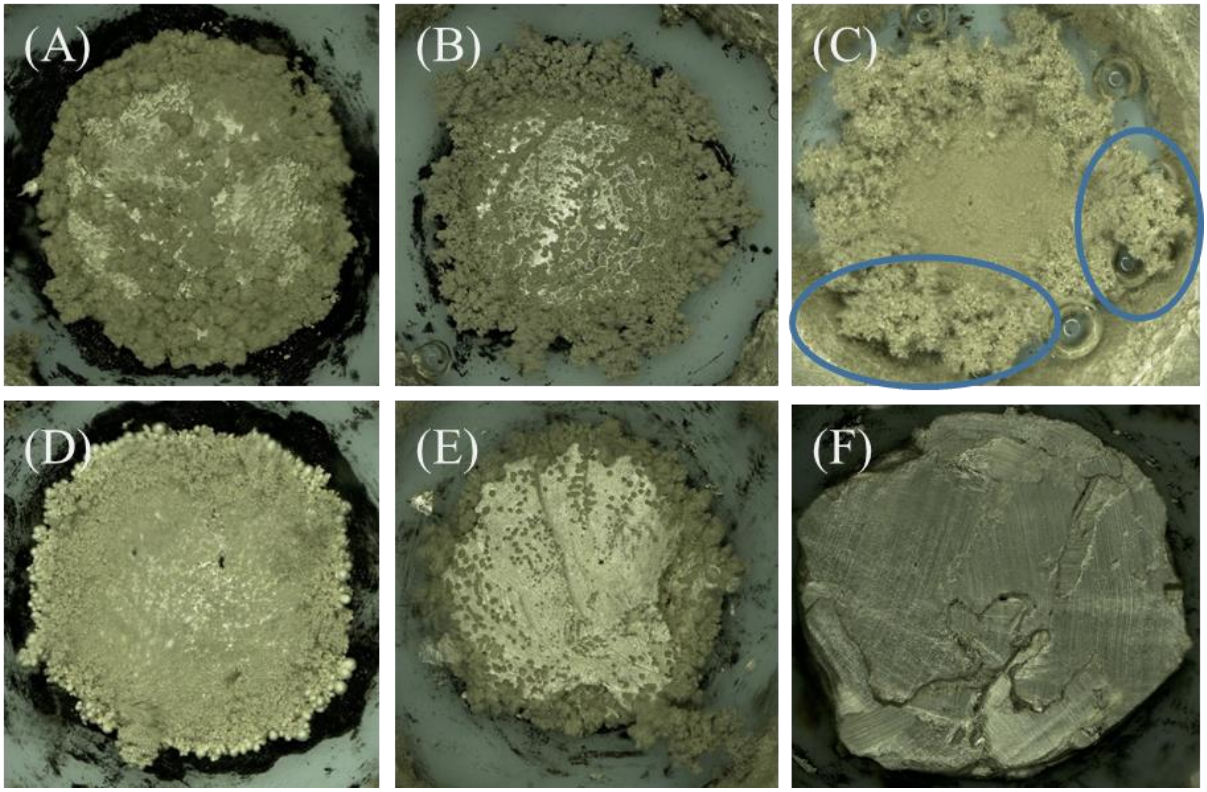

Figure 4 The optical photographs (each photograph was stitched together by lots of individual images with 100X magnification) of lithium electrodes with and without electrochemical deposition of lithium in different lithium salt electrolytes. (A) in 1 M LiBETFSi/DME/DOL electrolyte with deposition;(B) in 1 M LiClO4/DME/DOL electrolyte with deposition; (C) in 1 M LiDFOB/DME/DOL electrolyte with deposition; (D) in 1 M LiTFS/DME/DOL electrolyte with deposition; (E) in 1 M LiTFSi/DME/DOL electrolyte with deposition; (F) in 1 M LiTFSi/DME/DOL electrolyte without deposition. All electrolytes contain 0.1 M $LiNO_3$. The deposition condition is 2 mA for 1 hour.

In general, there are two types of dendrite morphologies in the micro scale as shown in figure 4 for different electrolytes: one is with lots of lithium wires (whiskers or needles) and structure is fluffy (not compact) as for LiDFOB electrolyte in figures 5(C) and 5(F); the other one is with lots of coarse or fine lithium particles and structure is compact as for other electrolytes in figures 4. Whisker-like lithium wires (or needles, as shown figures 5(C) and 5(F)) were also observed by others during the investigations of lithium deposition on different electrode surfaces and in different electrolytes, typically the lithium whiskers have a diameter of several um and a length in several hundred um range.[11, 21, 23- 26, 29, 30, 38] Based on the extensive studies of the whisker formation of Zn and Sn during electrochemical deposition[39,40], previously it's believed the lithium whisker formed in similar way in which the size of whisker increases through the accumulation of deposits in the base attached on the electrode instead of the tip away from the electrode[30]. However, this mechanism of whisker formation for lithium is debatable due to: 1, the whiskers of Zn and Sn were caused by the stress during electrochemical deposition; 2, the tip of the whisker always has the higher charge density and lithium ion diffusion rate that those on the bottom; 3, the in-situ observation (see videos and snapshot in figure S-1to S-5 in the supporting information) clearly shows the continuous increase of the tip of lithium whisker during electrochemical deposition.

Contrary to the whisker-like lithium deposits in LiDFOB electrolyte, in other lithium electrolytes the lithium deposits are composed of bush-like aggregates, [24, 31, 38] as shown in figures 4. At higher magnification (shown in figure 5), it can be observed that the bush-like aggregations are composed mainly by fine or coarse particles with some short whiskers. Due to the more compact structure of fine particles in other electrolytes, the overall size of the lithium dendrites in those electrolytes is much smaller than that in LiDFOB electrolyte. Since the only

difference of those electrolytes is the anions of the lithium salts, [38] the differences of dendrite morphologies clearly indicates the impact of different anions which was attributed to the different composition of the SEI (solid electrolyte interphase) layer on thesurface of the lithium electrode. [1, 2, 4-9, 11]

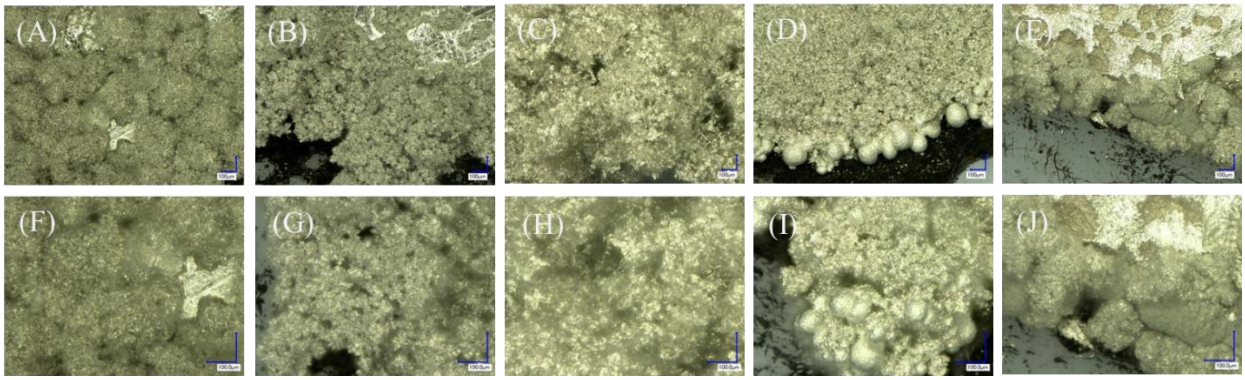

Figure 5 The optical photographs of lithium electrodes with and without electrochemical deposition of lithium in different electrolytes. In 1 M LiBETFSi/DME/DOL electrolyte with deposition, (A) and (F); in 1 M $LiClO_4$/DME/DOL electrolyte with deposition, (B) and (G); in 1 M LiDFOB/DME/DOL electrolyte with deposition, (C) and (H); in 1 M LiTFS/DME/DOL electrolyte with deposition, (D) and (I); in 1 M LiTFSi/DME/DOL electrolyte with deposition, (E) and (J). All electrolytes contain 0.1 M $LiNO_3$. The deposition condition is 2 mA for 1 hour. From (A) to (E), in 200X magnification; from (F) to (J) in 400X magnification.

Xiao Jie [42] wrote that a Cs salt could act as an additive in the electrolyte of the batteries could be used to reduce the dendrite growth. So one experiment as figure 6 shown is designed to find the effect of the Cs salt. In this experiment, four different Cs salts were used, CsNO3, CsClO4, Cs2CO3 and Cs2 (Oxlate). The results are shown on C D E and F in the figure 6. The first two are the sample without additive and with lithium nitrate. From the picture it could be found that the different Cs salts will lead to different structure and shape of the dendrites formation. The C with CsNO3 is moss like and it shape is closed pack. But for the other figures, the structure is loose and bush like. That still proves the anion of the salt is the dominant reason to determine the dendrite formation shape and growth rate. The Cs in this experiment does not affect the dendrite growth and formation as the Xiao demonstrates. The reason that cause the difference is maybe due to the current density difference at the deposition procedure. This experiment's current density is higher than the Xiao's. In the future, operating the charging process in a lower current density is another plan for further research.

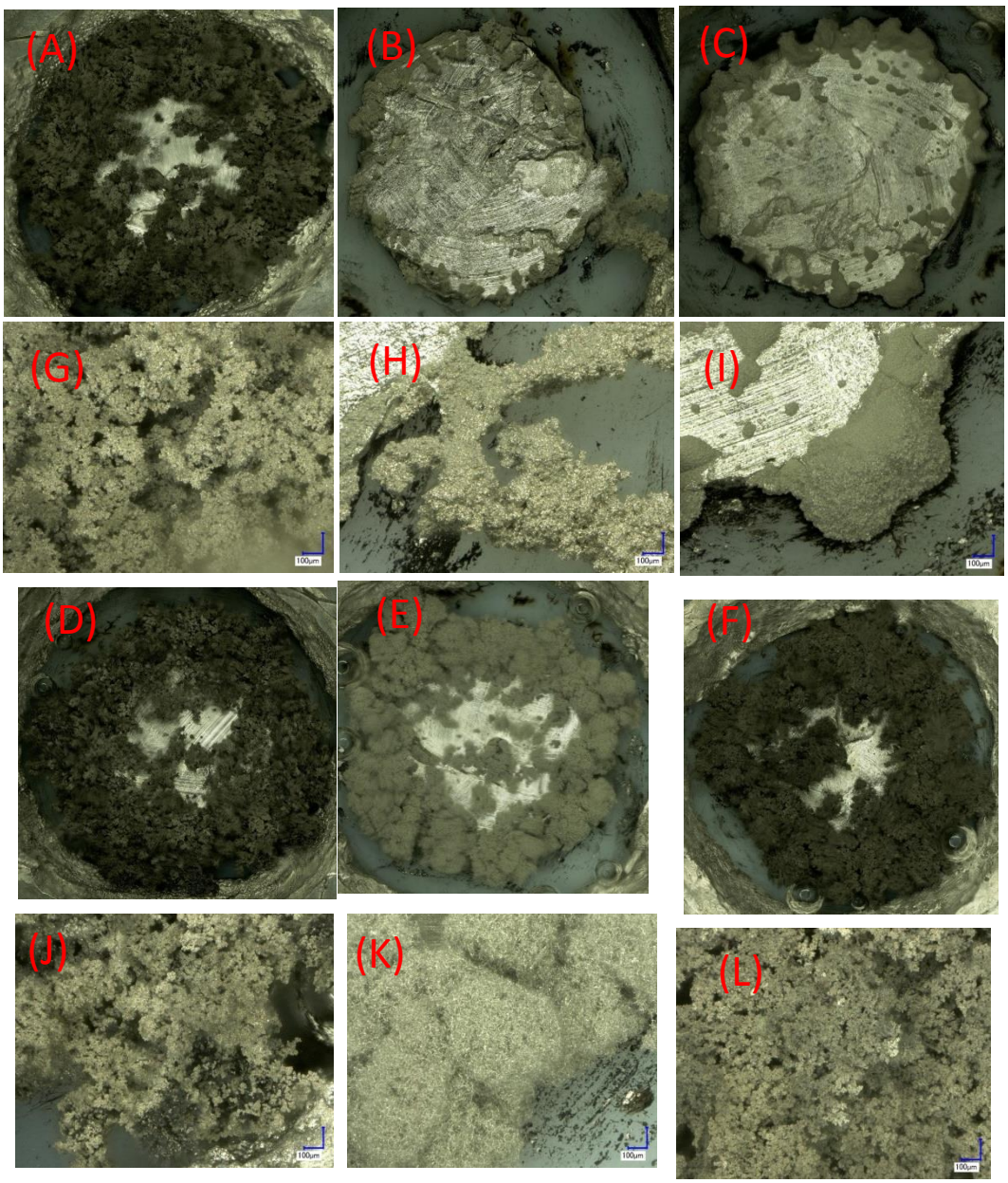

Figure 6. The optical photographs of lithium electrodes with and without electrochemical deposition of lithium in different electrolytes. In 1 M LiBETFSi/DME/DOL electrolyte with deposition, (A) and (G); In 1 M LiTSFi/DME/DOL, with 0.3M LiNO3 with deposition, (B) and (H); In 1 M LiTFSi/DME/DOL, with 0.1M CsNO3 with deposition, (C) and (I); In 1 M LiTFSi/DME/DOL, with 0.1M CsClO4 with deposition, (D) and (J); In 1 M LiTFSi/DME/DOL, with 0.05M Cs2CO3 with deposition, (E) and (K); In 1 M LiTFSi/DME/DOL, with 0.05M Cs2(Oxalate) with deposition, (F) and (L). The deposition condition is 2 mA for 1 hour. From (A) to (F), in 100X stitching magnification; from (G) to (L) in 200X magnification.

Figure 7 is another experiment in which the purpose is to find the transition metal salts' effect on dendrite growth. Bismuth (Bi), Indium (In), Lead (Pb) and Cobalt (Co) were chosen as the transition metal and nitrate has been chosen as the salt. Those metal salts will react with lithium and form a thin metal layer which acts like a shell on the lithium electrode. When the deposition of the lithium is happening, it will deposit on the lithium electrode plane which is under the metal shell. So the metal shell could act as a cover and compress the growing dendrites controlling the dendrite morphology and size in order to prevent dendrite overgrowth. From the figure 7, it can be observed that B C D, the color of the electrode has been changed, which means there is some reaction between the salts and the lithium salt and electrode. The reaction formed a thin layer of the metal deposition on the lithium electrode surface. But from the picture after the deposition, it can be found that the dendrites are still grown on the newly formed metal-surface. This means that the use of the thin metal film to control the dendrite growth failed in this environment. For the C and E figure, the dendrite formation is similar to the first sample with $LiNO_3$ and the dendrite shape is also similar. The Cobalt (II) phthalocyanine did not react with lithium metal, the deposition still happened on the lithium electrode surface. That makes the result similar to the blank samples without additives.

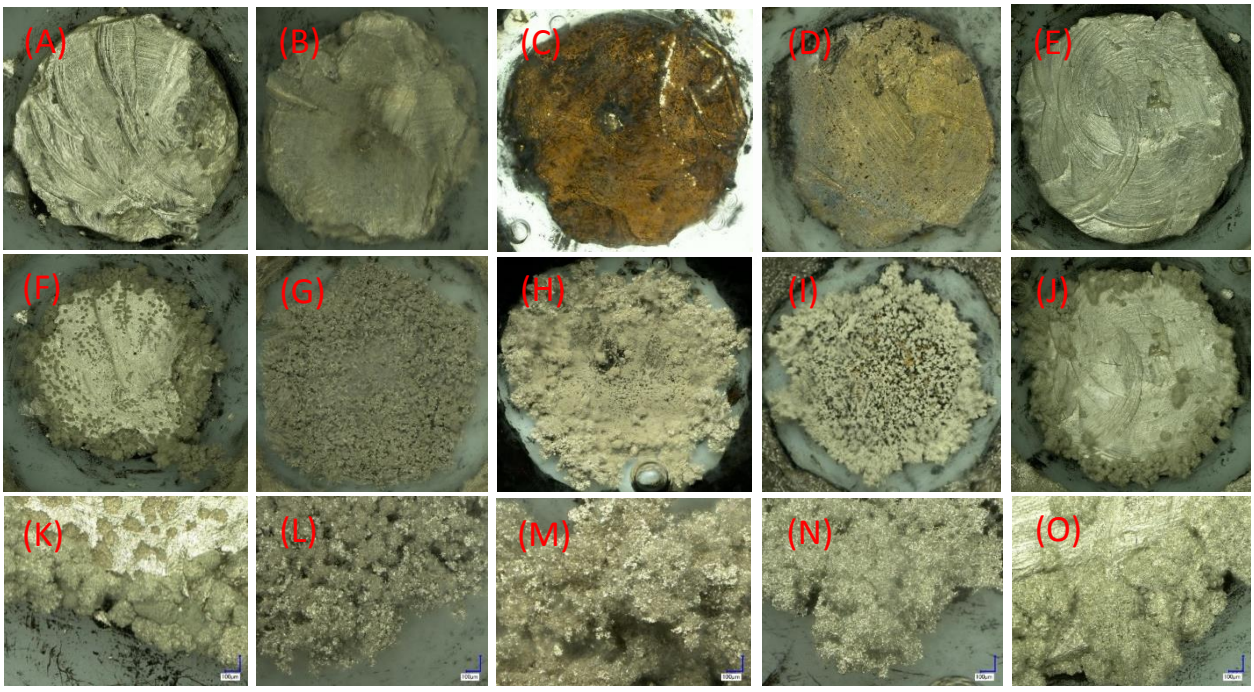

Figure 7. The optical photographs of lithium electrodes with and without electrochemical deposition of lithium in different electrolytes. In 1 M LiBETFSi/DME/DOL electrolyte with 0.1 M LiNO3 before and after deposition, (A),(F) and (K); In 1 M LiTSFi/DME/DOL, with 0.1M LiNO3 and 0.05M Bi(NO3)3 before and after deposition, (B),(G) and(L); In 1 M LiTSFi/DME/DOL, with 0.1M LiNO3 and 0.05M In(NO3)3 before and after deposition (C), (H) and (M); In1 M LiTSFi/DME/DOL, with 0.1M LiNO3 and 0.05M Pb(NO3)2 before and after deposition, (D),(I) and (N); In 1 M LiTFSi/DME/DOL, with 0.1M LiNO3 and 0.025M Co(II) phthalocyanine before and after deposition. The deposition condition is 2mA for 1hour. From (A) to (J), in 100X stitching magnification; from (K) to (O) in 200X magnification.

In order to investigate the effect of charging current density on the dendrite growth. 3 different current densities were applied to the cell. Figure 8 shows the dendrite growth in Lithium sulfur battery at different currents. In order to keep the total capacity the same, the charging time have been modified due to the different current. For 2mA current the charging time is 1 hour. For the 0.8mA current the time is 2.5 hour. For the 0.1 mA the charging time is 20 hours. In order to avoid the leakage of the cell, the 20-hour experiment is finished in the argon glove box. From the figures (A) (B) and (C), the size of the dendrite deposition on the cell has a significantly shrinkage when operated at a low current density. That means the current density of the charging process is one of the element that affects the dendrite growth. Also the cesium salt CsNO3 was introduced as additive of the electrolyte for comparison. The shape and size of the dendrite are not changed when compared to the samples without CsNO3. But on the picture, it is observed that the structure of the dendrites become well-packed and the size becomes small when adding the cesium nitride. So the Cesium still has some benefit for controling the dendrite growth but not as much as the changing of the current density. Lower current density will be applied to the battery to see the change in future experiments.

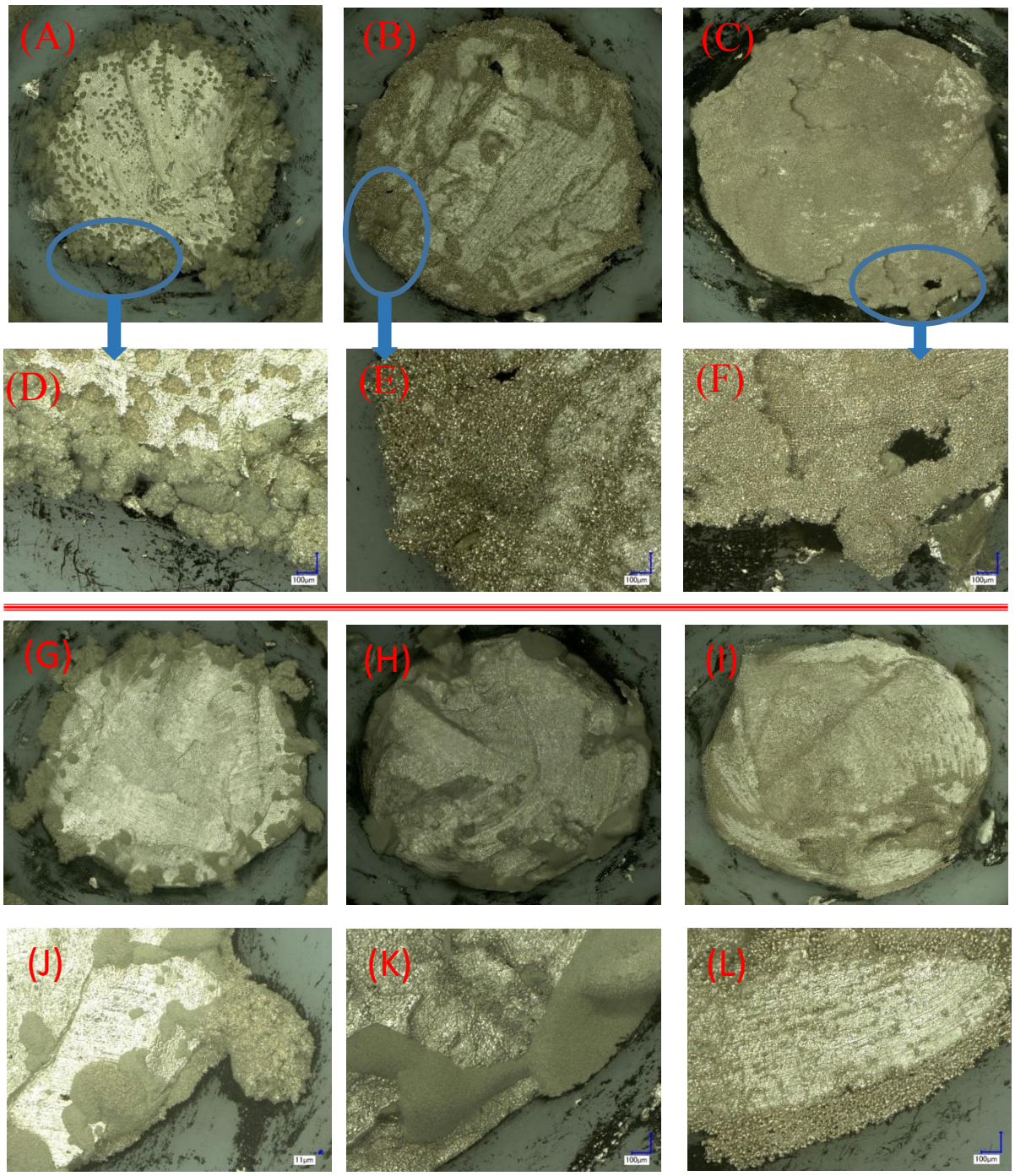

Figure 8. The optical photographs of lithium electrodes with electrochemical deposition of lithium in LiTFSi/DME/DOL, with 0.1M LiNO3, with different current. In 2mA for 1hour, (A) and (D); In 0.8mA for 2.5 hour, (B) and (E); In 0.1mA for 20 hours, (C) AND (F). 0.05M CsNO3 is added to the electrolyte from (G) to (L). In 2mA for 1hour, (G) and (J); In 0.8mA for 2.5 hour, (H) and (K); In 0.1mA for 20 hours, (I) AND (L). From (A) to (C) and (G) to (I), in 100X stitching magnification; from (D) to (F) and (J) to (L) in 200X magnification.

Figure 9 is another experiment which was designed to investigate the effect of the additive in the electrolyte to the dendrite growth. In figure A is LiDFOB/DME/DOL with LiNO3 as additive in the electrolyte. For the B, 0.05 M CsNO3 is added to the electrolyte compare to the first one. From the result it could be find the size of the dendrite is smaller when adding the CsNO3 than just use LiNO3 as the additive of the electrolyte. Also the dendrite shape is closed-packed and moss-like. That is also proof that CsNO3 has some effect in reducing the size of the dendrite growth. In the future more electrolytes will be tested like LiBETFSI to observe the Cs salt additive performance.

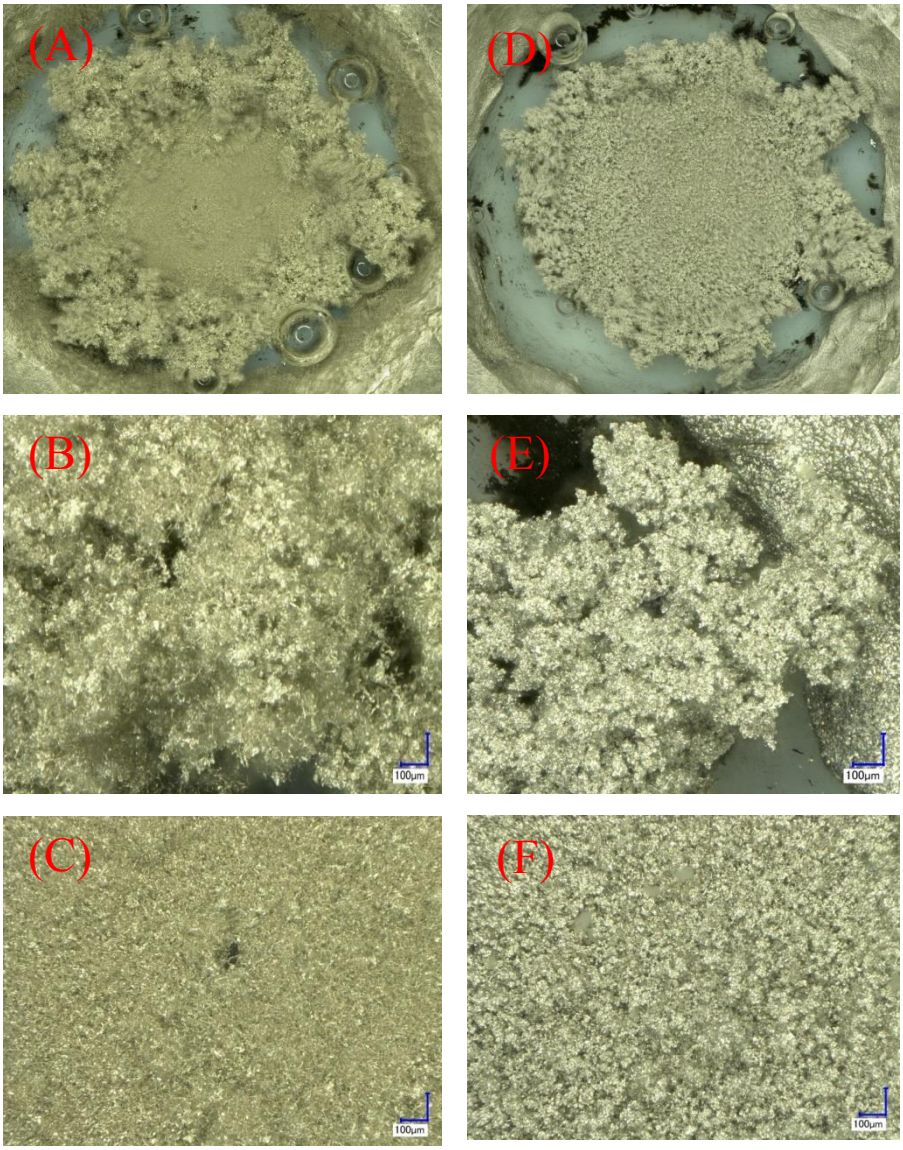

Figure 9. The optical photographs of lithium electrodes with electrochemical deposition of lithium in 1 M LiDFOB/DME/DOL, with 0.1 M LiNO3 after deposition,(A),(B) and (C). In 1M LiDFOB/DME/DOL, with 0.1 M LiNO3 and 0.05 M CsNO3 after depostition, (D), (E) and (F). The deposition condition is 2mA for 1 hour. (A) and (D), in 100X stitching magnification. (B),(C),(E) and (F), in 200X magnification.

In the second part of the experiment, the structure of the LiDFOB, LiBF4 and LiBOB is given in figure 1. The LiDFOB structure is the combination of the LiBF4 and LiBOB. In order to research the anion structure and component effect to the dendrite growth, three salt were added as electrolyte and deposit in 2 mA current for 1 hour. The result is in Figure 10. The size of the dendrite in LiBOB is the largest string-like dendrites with some condensed lithium particles adhere on the strings. The dendrite size of the LiBF4 is the smallest and it is bush-like structure. The size of dendrite of the LiDFOB is between the other two and it can be found the similar structures and morphologies from the other two lithium salt's dendrites. So this comparison prove the result that different anion will impact the different composition and dendrite shape in surface SEI layer on the lithium electrode. [1, 2, 4-9, 11]

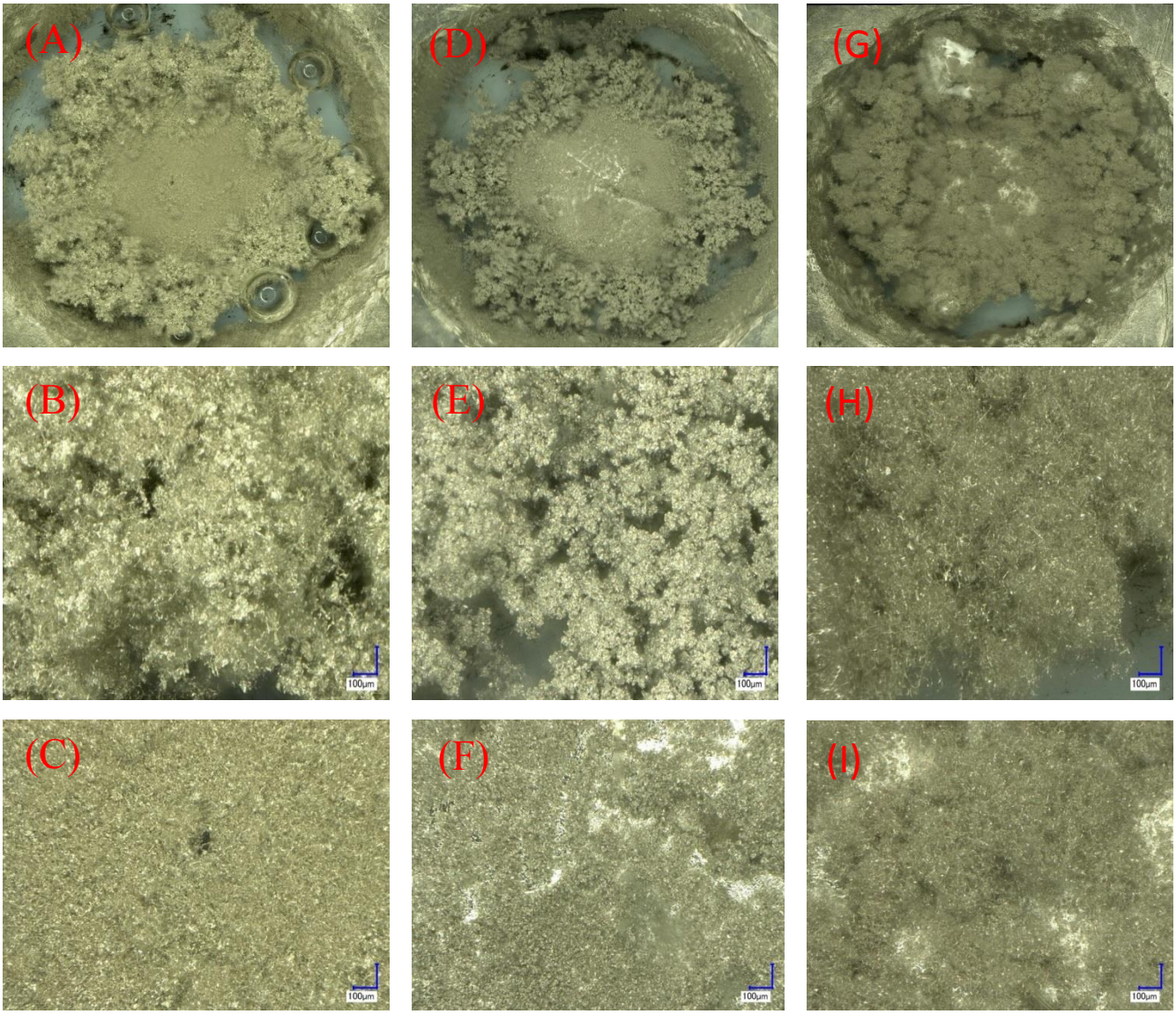

Figure 10. The optical photographs of lithium electrodes with electrochemical deposition of lithium in 1 M LiDFOB/DME/DOL, with 0.1 M LiNO3 after deposition, (A), (B) and (C). In 1 M LiBF4/DME/DOL, with 0.1 M LiNO3 after deposition, (D), (E) and (F) after deposition; In 1 M LiBOB/DME/DOL, with 0.1 M LiNO3 after deposition, (G), (H) and (I). The deposition condition is 2mA for 1hour. (A), (D) and (G) in 100X stitching magnification. The rest are in 200X magnification

Although lots of efforts have been done on understanding the reasons for the dendrite formation during lithium deposition, [3-32, 38] obviously the full picture for the dendrite formation is still unavailable now. Generally, most (if not all) of the research work just points out the chemical and electrochemical conditions that could influence the dendrite formation, such as the different type of lithium salts and solvents, [4, 6, 8, 9, 11, 14, 15, 18, 28, 38] the different concentration of lithium salts, [8, 27, 29, 38] the deposition current densities, [14, 15, 18, 24, 27, 29] and the different deposition temperature [14, 29, 31]. In this work, similar results were observed. For example, an experiment with different solvent is designed. From the Figure 11 it could be found that the shape of the dendrite formation is different when using different solvent. There are some bubbles generate in the (D), it could be found that the DMSO is react with the lithium. From the sigma manual of the DMSO and Deyang [33], it can be found that it reacts with metals and generate a mixture of hydrogen and methane gases at the cathode. At higher magnification, the G will grow moss-like dendrites which has packed structure and the other dendrites are loose and large. The dendrites in the H is closer to the shape in the G because the solvent is the 1:1 DOL and DME mixture. As the figure 10 shown, it can be concluded that the solvent affects the growth of the dendrite during the charging process of the lithium sulfur batteries. For 1 M LiTFSi salt in different solvents (in pure DME, in pure DOL, and in 1:1 mixture, result shown in figure 12), in pure DOL solvent, the dendrite morphology is filled with big chunky deposit; in pure DME solvent, the dendrite morphology is filled with fine-particle deposit; and in 1:1 mixture solvent, the dendrite morphology is a mixture of big chunky deposit and fine-particle deposit. For different concentration of LiTFSi in DME/DOL mixture (0.5 M, 1.0 M, and 2.0 M), the more compacted dendrite morphology is favorably formed in the electrolyte with higher concentration of LiTFSi salt as shown in figure S-7 (in supporting

information), although the overall dendrite formation is no big difference. Some publications reported similar observation for dendrite formation in different concentration of electrolyte [8, 38], however one publication reported more dendrite formation in higher concentration of electrolyte [29] and another publication reported less dendrite formation in higher concentration of electrolyte [41]. For deposition current density, three different current densities were compared as shown in figure S-8. Clearly, for the same geometrical lithium electrode, as the deposition currents increase from 0.1 mA to 2mA, the dendrite formation as well as the homogeneity of the lithium deposition is more evident in the deposition with higher current. Similar observations were reported by Ota *et al* [14]and Gireaud *et al* [15], although Fukunaka *et al* reported big dendrites formed at extremely low deposition current density [29].

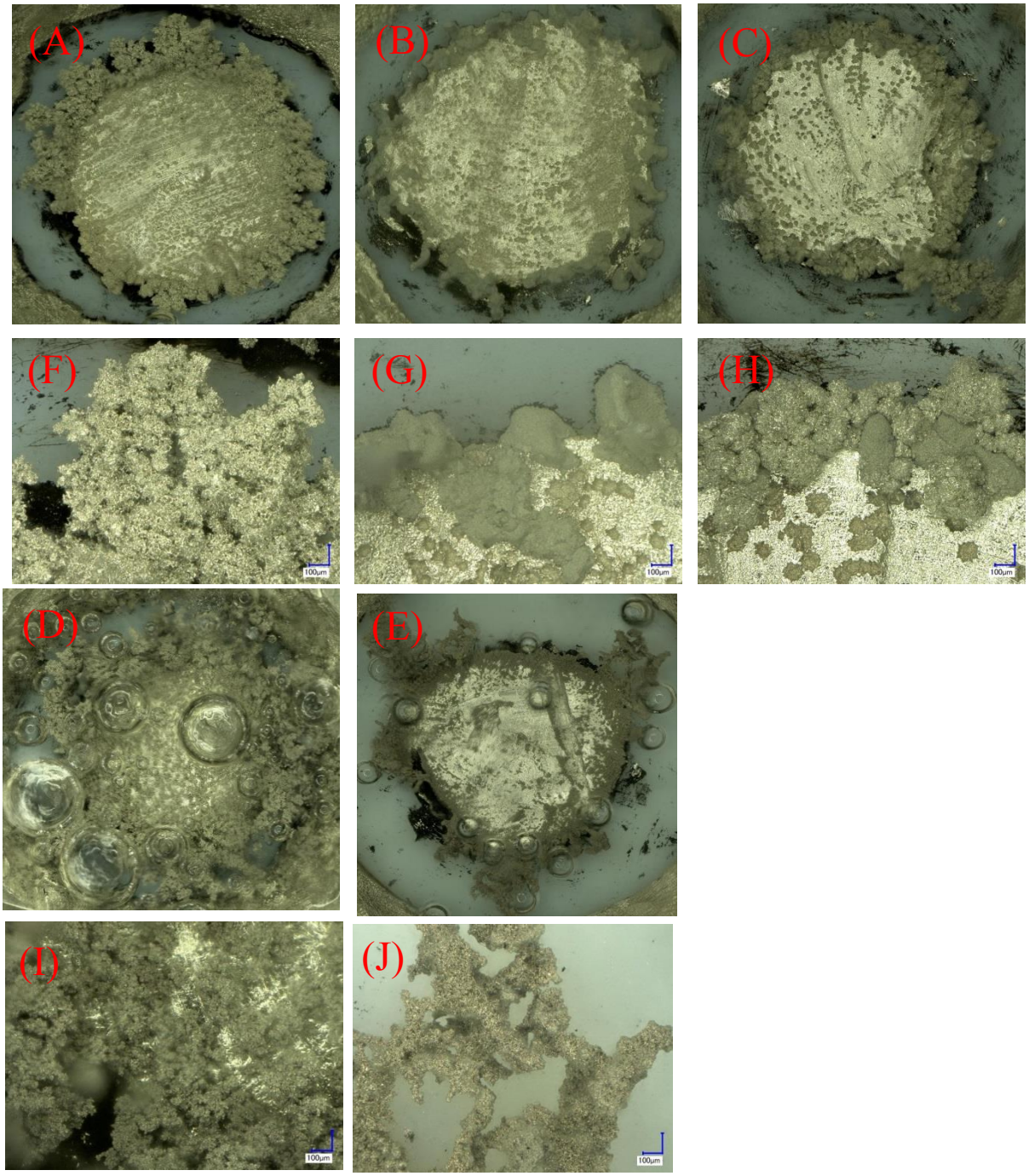

Figure 11 The optical photographs of lithium electrodes with electrochemical deposition of lithium in 1M LiTFSi with 0.1M LiNO3, In pure DOL after deposition, (A) and (F); In 1M LiTFSi with 0.1M LiNO3, In pure DME after deposition, (B) and (G); In 1M LiTFSi with 0.1M LiNO3, in 1:1 mixture after deposition, (C) and (H); In 1M LiTFSi with 0.1M LiNO3, In pure DMSO after deposition, (D) and (I); In1M LiTFSi with 0.1M LiNO3, In pure AND after deposition (E) and (J). The deposition condition is 2mA for 1 hour. (A) to (E) are in 100X stitching magnification. (F) to (J) are in 200X magnification.

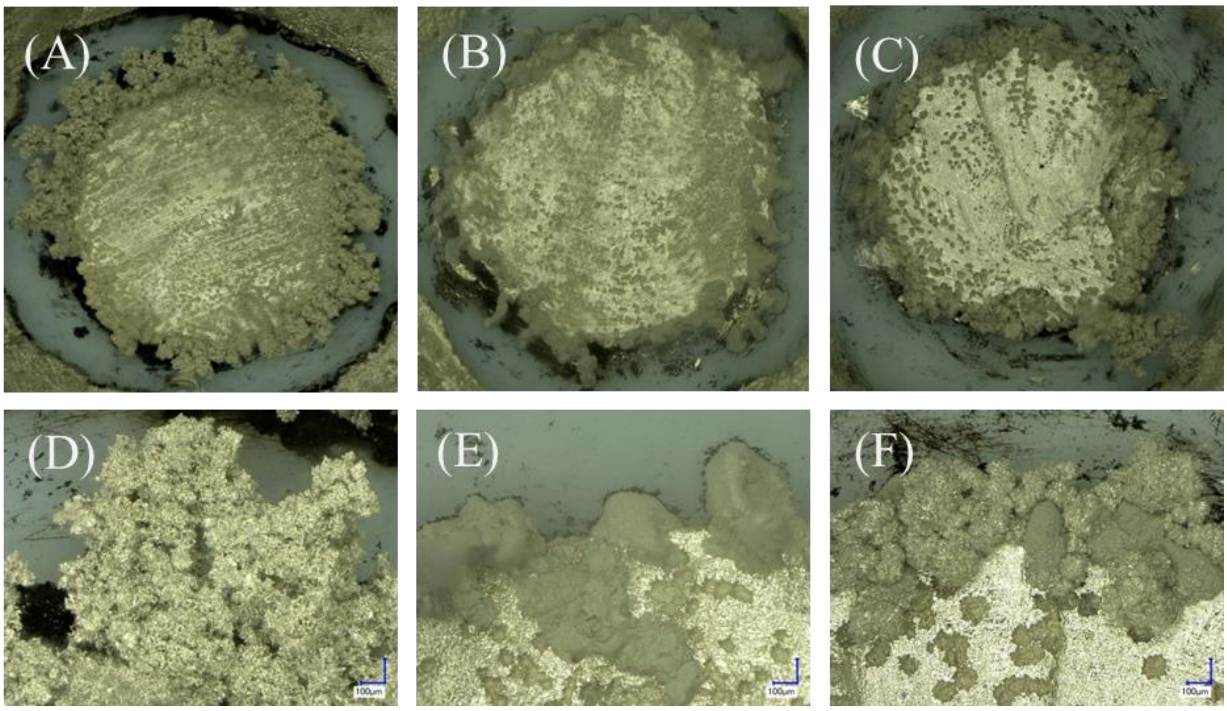

Figure 12 Baseline electrolyte of LiTFSi in pure DOL (A), in pure DME (B), and in DME/DOL (1:1) mixture (C).

3.2 Lithium dendrite morphology in electrolytes with lithium polysulfide.

To simulate the electrolyte condition in Li-S battery which normally contains elemental sulfur and different polysulfide species, 25 mM polysulfide mixture was added into the baseline electrolytes by mixing the Li_2S and S_8 in stoichiometric ratio of Li_2S_6. Although all solids of Li_2S and S_8 in the electrolytes disappeared and homogenous dark brown solutions were formed after thoroughly mixing, different polysulfide species as well as elemental sulfur were in the electrolytes instead of just Li_2S_6.[33] It's been reported that the existence of polysulfide species in the electrolyte could suppress the dendrite formation during lithium deposition due to the passivation of the dendrite surface through reaction between polysulfide species and the newly deposited lithium.[17, 32, 36] Figure 13 shows the surface morphology of lithium electrode after deposition at 2 mA for 1 hour in the electrolytes with 25 mM polysulfide species. As shown in figure 4, big dendrites are formed in all different electrolytes with polysulfide species at that deposition condition. Compared with figure 13 for the baseline electrolytes without polysulfide species, the suppression effect of polysulfide species on lithium dendrite formation is not that evident in figure 13. Since the argument for the suppression effect of polysulfide species is based on the reaction between polysulfide species and the newly deposited lithium, it's debatable. First, due to the addition of $LiNO_3$ in the electrolyte, the direct shuttle reaction between lithium and polysulfide species was greatly inhibited [33], thus the potential products through the shuttle reaction, such as Li_2S and Li_2S_2 may not form on the dendrite surface. Second, to really passivate the dendrite surface and suppress the deposition of lithium on dendrite surface, the SEI layer must be thick enough and the side reaction to form the thick SEI layer must be fast enough compared to the electrochemical deposition. If this assumption is true, then the columbic efficiency should be low. However, in our recent work, it was demonstrated that even at low

discharge/charge rate of Li-S battery the columbic efficiency is high. [37] And that observation clearly indicates the above assumption is not true during lithium deposition in Li-S battery. The snap-shots at different deposition time for both electrolytes without polysulfide and electrolytes with polysulfide were summarized in figures S-9 to S-13, it can be seen in those figures both electrolytes have similar dendrite formation kinetics and there is no observable suppression effect for electrolytes with polysulfide.

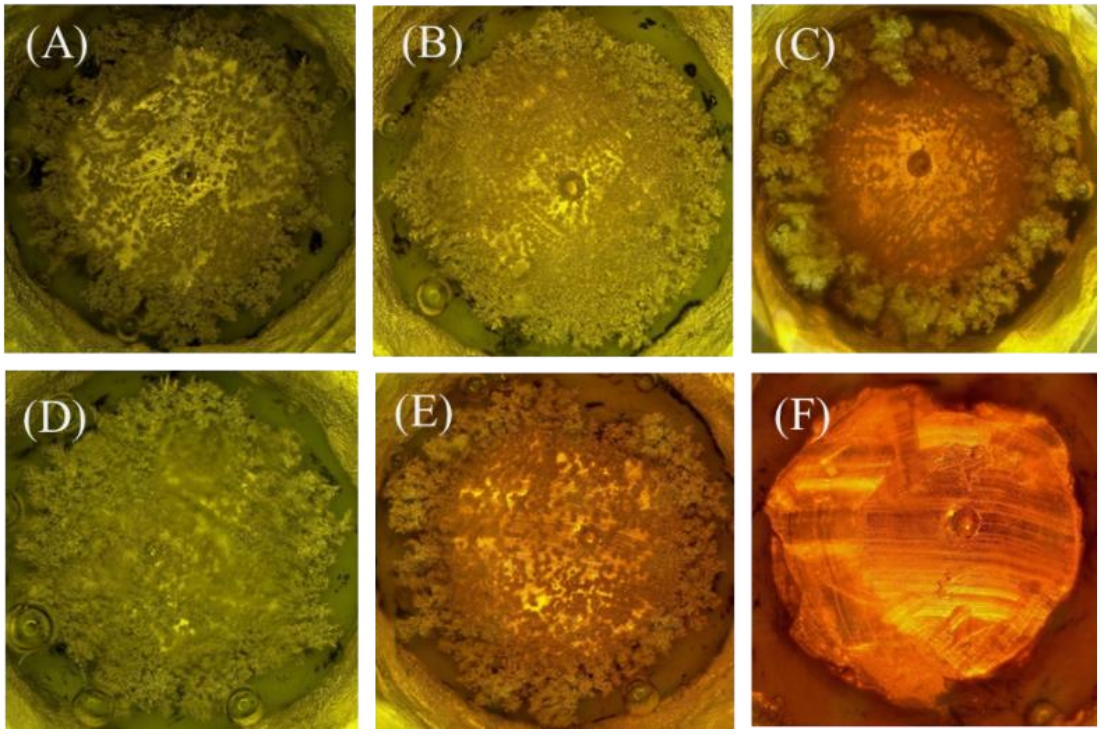

Figure 13 The optical photographs (each photograph was stitched together by lots of individual images with 100X magnification) of lithium electrodes with and without electrochemical deposition of lithium in different electrolytes. (A) in 1 M LiBETFSi/DME/DOL electrolyte with deposition;(B) in 1 M LiClO4/DME/DOL electrolyte with deposition; (C) in 1 M LiDFOB/DME/DOL electrolyte with deposition; (D) in 1 M LiTFS/DME/DOL electrolyte with deposition; (F) in 1 M LiBETFSi/DME/DOL electrolyte with deposition; (E) in 1 M LiTFSi/DME/DOL electrolyte with deposition; (F) in 1 M LiTFSi/DME/DOL electrolyte without deposition. All electrolytes contain 0.1 M $LiNO_3$ and 25 mM lithium polysulfide (Li_2S_6 in stoichiometry). The deposition condition is 2 mA for 1 hour.

Although the suppression effect for electrolyte with polysulfide is hard to be observed, the existence of polysulfide in the electrolytes does have some effects on the morphology of dendrite in micro-scale at least in some cases as shown in figure 14. Compared figure 14 with figure 5, two observations can be easily found. First, for electrolytes with $LiClO_4$ and LiDFOB, the existence of polysulfide species in the electrolytes has limited effect on the micro-structure of the dendrite morphology. The micro-structures of the dendrites formed in these two electrolytes with and without polysulfide species are almost the same as shown figures 5 and 14. For example, for electrolyte of $LiClO_4$, the micro-structures in figure 14(G) (with 25 mM polysulfide) and in figure 5(G) (without polysulfide) are both composed of compacted coarse particle-like deposition. Second, for electrolytes with LiBETFSi, LiTFS, and LiTFSi, the existence of polysulfide species in the electrolytes has noticeable effect on the micro-structure of the dendrite morphology. For instance, for electrolyte of LiTFS, the micro-structures in figure 14(I) (with 25 mM polysulfide) and in figure 5(I) (without polysulfide) are totally different, one is with spike-like deposition, the other one is with sphere-like deposition. These two interesting observations clearly show the complexity of dendrite formation, and the reason for those is beyond the topic of this work.

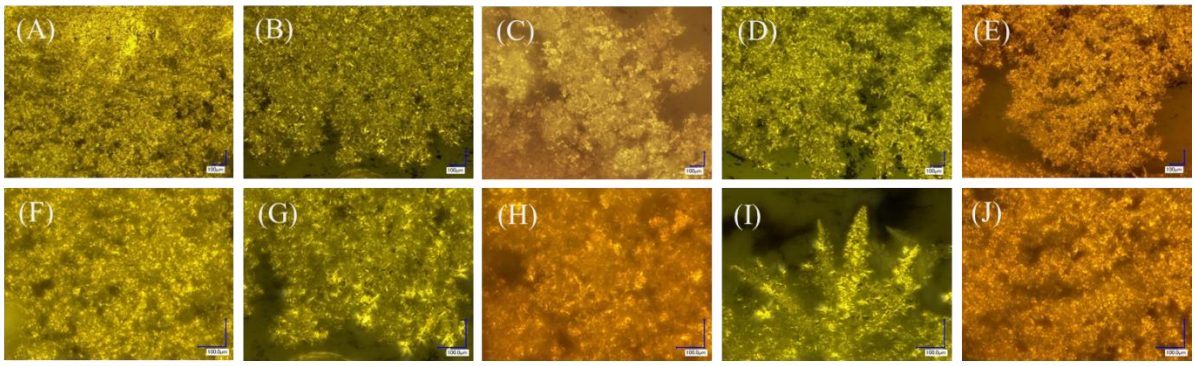

Figure 14 The optical photographs of lithium electrodes with electrochemical deposition of lithium in different electrolytes containing polysulfide species. In 1 M LiBETFSi/DME/DOL electrolyte with deposition, (A) and (F); in 1 M $LiClO_4$/DME/DOL electrolyte with deposition, (B) and (G); in 1 M LiDFOB/DME/DOL electrolyte with deposition, (C) and (H); in 1 M LiTFS/DME/DOL electrolyte with deposition, (D) and (I); in 1 M LiTFSi/DME/DOL electrolyte with deposition, (E) and (J). All electrolytes contain 0.1 M $LiNO_3$ and 25 mM lithium polysulfide (Li_2S_6 in stoichiometry). The deposition condition is 2 mA for 1 hour. From (A) to (E), in 200X magnification; from (F) to (J) in 400X magnification.

As discussed in baseline electrolyte without polysulfide, the deposition current density has critical effect on the dendrite morphology. Thus it's interesting to see if the deposition current density has similar effect in the electrolyte with polysulfide. Figure 15 shows the surface morphology of lithium deposition in 1 M LiTFSi/DME/DOL with 0.1 M $LiNO_3$ and 25 mM polysulfide at different deposition currents, 0.1 mA, 0.8mA, 2mA. Obviously, the current density also has some effects on the dendrite formation in the electrolyte with polysulfide, the dendrite formation in 0.1 mA deposition current (as shown in figure 15(C) and (F)) is a little bit less than that in 2 mA deposition current (as shown in figure 15(A) and (D)). However, the difference of dendrite formation in high and low deposition currents is not that notable in electrolyte with polysulfide as in electrolyte without polysulfide as shown figure S-8. This observation confirms our previous observation again that the polysulfide species has no suppression effect on the dendrite formation.

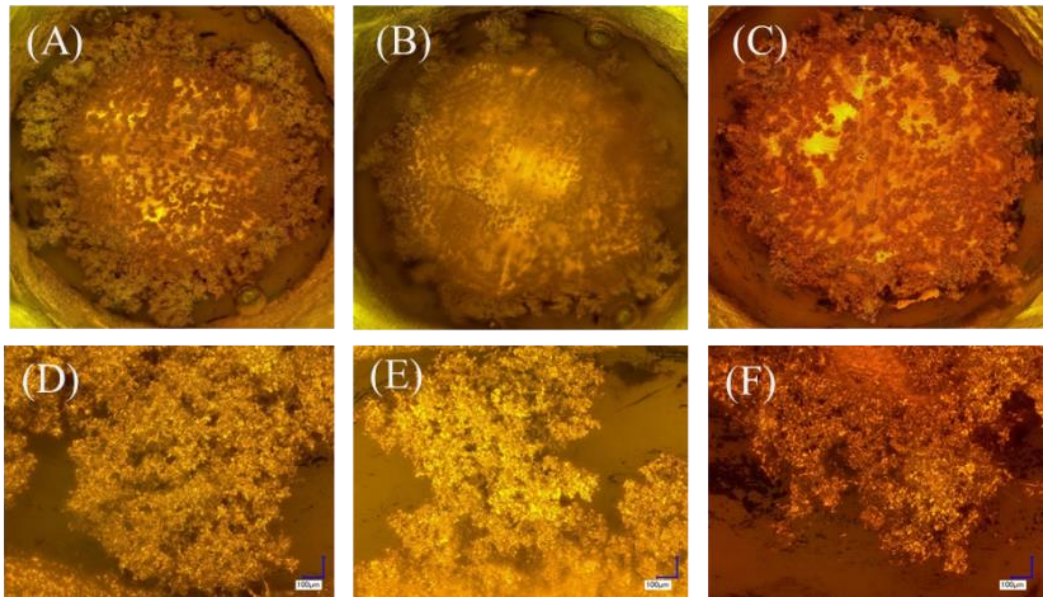

Figure 15 The optical photographs of lithium electrodes under different electrochemical deposition conditions. The electrolyte is 1M LiTFSi/DME/DOL containing 0.1 M $LiNO_3$ and 25 mM lithium polysulfide (Li_2S_6 in stoichiometry). 2 mA and 1-hour deposition for (A) and (D); 0.8 mA and 2.5-hour deposition for (B) and (E); 0.1 mA and 20-hour deposition for (C) and (F). From (A) to (C), in 100X magnification; from (D) to (F) in 200X magnification.

Recently, to minimize the dendrite formation on lithium anode during lithium deposition, additive in electrolyte and modification of lithium anode were also investigated in some research work. For example, Zhang *et al* [42] first reported that by adding cesium salts into the electrolyte the dendrite-free deposition of lithium is achieved through self-healing electrostatic shield (SHES) mechanism; Dunn *et al* [34] first reported that by coating the lithium anode with organic tetraethoxysilane (TEOS) the lithium electrode is dendrite-free for over 100 cycles of stripping and plating due to the stabilization of lithium surface by silicate film. Based on those promising strategies [34, 42], in this work we also investigated the feasibility of those strategies in suppression lithium dendrite in Li-S condition. Figures 16(B) and 16(E) show the dendrite morphology formed in the electrolyte of 1 M LiTFSi/DME/DOL with 0.1 M $LiNO_3$, 25 mM polysulfide, 50 mM $CsNO_3$. Figures 16(C) and 16(F) show the dendrite morphology formed in the electrolyte of 1 M LiTFSi/DME/DOL with 0.1 M $LiNO_3$, 25 mM polysulfide, 50 mM $CsNO_3$ after the electrode treated with TEOS. Compared with the dendrite morphology in figures 16 (A) and 16(D) which is obtained in the of 1 M LiTFSi/DME/DOL with 0.1 M $LiNO_3$ and 25 mM polysulfide without coating on the lithium electrode, there is no big difference for the morphologies of lithium dendrite obtained under different conditions. However in a recent Li-S research work by Choi *et al* [43], it's demonstrated that adding cesium nitrate ($CsNO_3$) into the electrolyte of a modified Li-S battery could prevent the dendrite growth based on SHES mechanism, the cross-sectional SEM images of the lithium disk electrode in a coin cell set-up clearly show a much thicker lithium dendrite in electrolyte without $CsNO_3$. The possible reasons for this different observation could be from different electrochemical cell set-up and different electrochemical operation condition. For electrochemical cell set-up: in this work, in the self-made electrochemical cell, the lithium from electrochemical deposition can freely accumulate

without any physical barrier and disturbance; in Choi's work [43], the separator could be a physical barrier and potentially could disturb the lithium accumulation. For electrochemical operation condition: in this work, the deposition current density is about 10 $mA*cm^{-2}$ (2mA on the electrode with about 5mm ID); in Choi's work, the deposition current density is about 0.84 $mA*cm^{-2}$, [43] which is much less than our current density. These two reasons could be also used to explain why TEOS coating didn't work in this work but it did work in Dunn's work [34]. At this point, someone may question about the high current density used in this work. However, it was already pointed out that for a practical Li-S battery with energy density higher than that of current lithium-ion battery, the sulfur loading must be over 2.0 $mg*cm^{-2}$. [44-47] Based on that, the 1C rate of Li-S battery with 2.0 $mg*cm^{-2}$ sulfur loading will result in a current density about 3.4 $mA*cm^{-2}$. Moreover, nowadays there are lots of publications with sulfur loading close or over 10 $mg*cm^{-2}$, [47-50] and also faster charge rate is always preferred in practical application of rechargeable battery, the current density in this work is pretty reasonable.

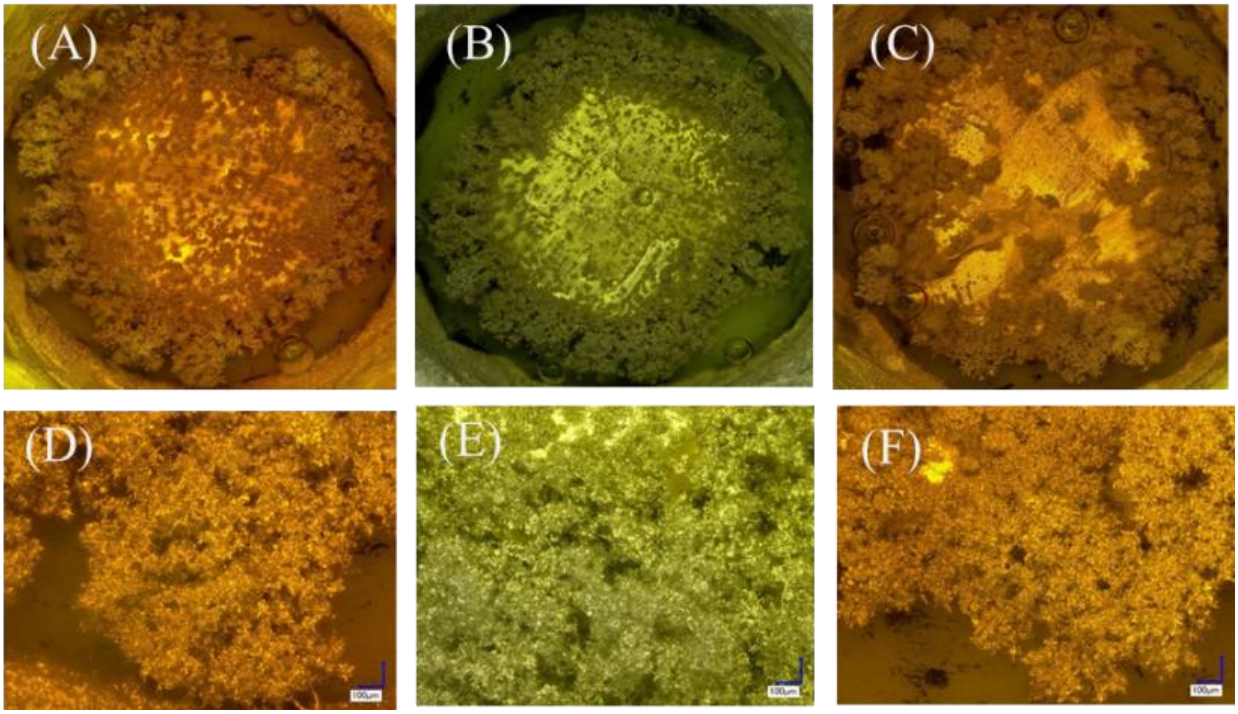

Figure 16 The optical photographs of lithium electrodes after electrochemical deposition with and without additives. All electrolytes are 1M LiTFSi/DME/DOL containing 0.1 M $LiNO_3$ and 25 mM lithium polysulfide (Li_2S_6 in stoichiometry). (A) and (D), for electrolyte without any additive; (B) and (E), for electrolyte with 50 mM $CsNO_3$ (99.99%)in electrolyte; (C) and (F), for electrode coated with tetraethyl orthosilicate (TEOS,99.999%) and electrolyte with 50 mM $CsNO_3$.From (A) to (C), in 100X magnification; from (D) to (F) in 200X magnification. The deposition condition is 2 mA for 1 hour.

4. Future work

In summary, a reliable and straightforward optical microscopic method for *in-situ* monitoring of lithium dendrite formation in electrolytic conditions as in a Li-S battery was successfully applied in this work. The observation of the dendrite growth of the Lithium-Sulfur battery is still in its early stages and the next step could be to increase the scope of this research by using different materials and methods.

In this thesis we only discussed using lithium as the substrate of the dendrite growth. By changing the design of the two-electrode cell, we could change the substrate to other materials like cooper, aluminum, lead and indium in order to see the effects the substrate will have on the lithium deposition and dendrite growth.

Further investigation into the solvent is another future research direction for future. We could use more organic solvent like the Ethyl methyl carbonate, ethylene carbonate and propylene carbonate which are mainly used in current LiB batteries. Then we could expend our research field not only focus on the lithium sulfur batteries but also apply our previous result and knowledge to Lithium-ion batteries.

Also from Nishida [29], the lithium battery cell is designed in another way which the optical microscope observed the vertical side of the electrode. This method is easy to find out the dendrite growth morphology and dendrite length from the observation. Also the concentration of the lithium salt in the electrolyte and temperature is mentioned as an effect to control the dendrite growth when charging. So these are also considered as a future plan.

Also we could use X-ray photoelectron spectroscopy (XPS) to analysis the effect of the SEI layer formation on the deposition of lithium process because most research has considered that they have relationships. So in the future, more research work on suppressing the dendrite

formation in Lithium-Sulfur battery will be designed and operated. SEM (scanning electron microscope) is another way to observe the dendrite growth in the cell. Because of the high resolution of the SEM, we could even observe the SEI layer of the batteries and discover the relationship between those two structures. Those will be discovered in the future design of the experiments.

5. Supporting information

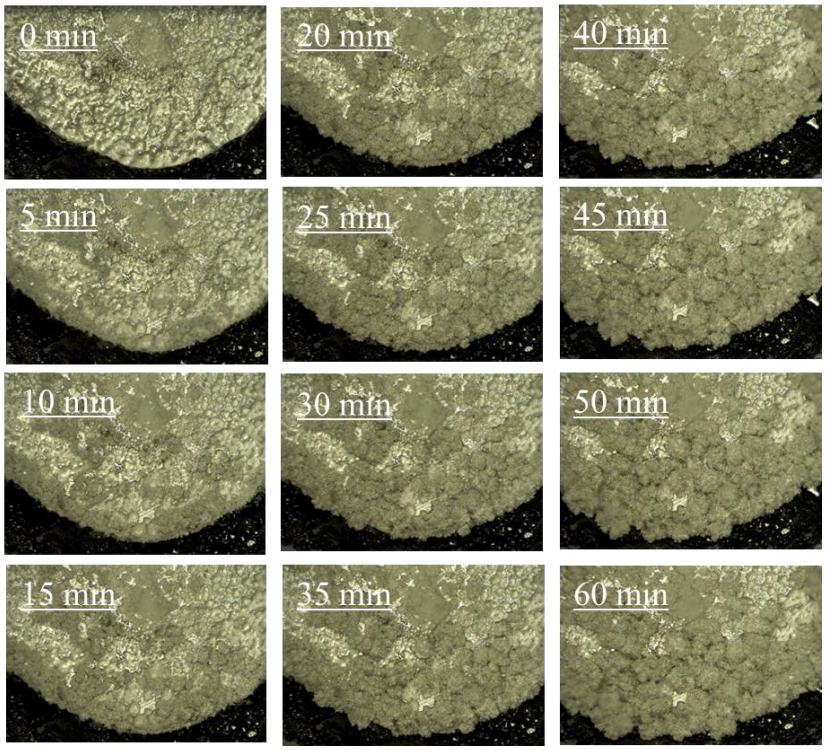

Figure S-1, Baseline electrolyte of LiBETFSi

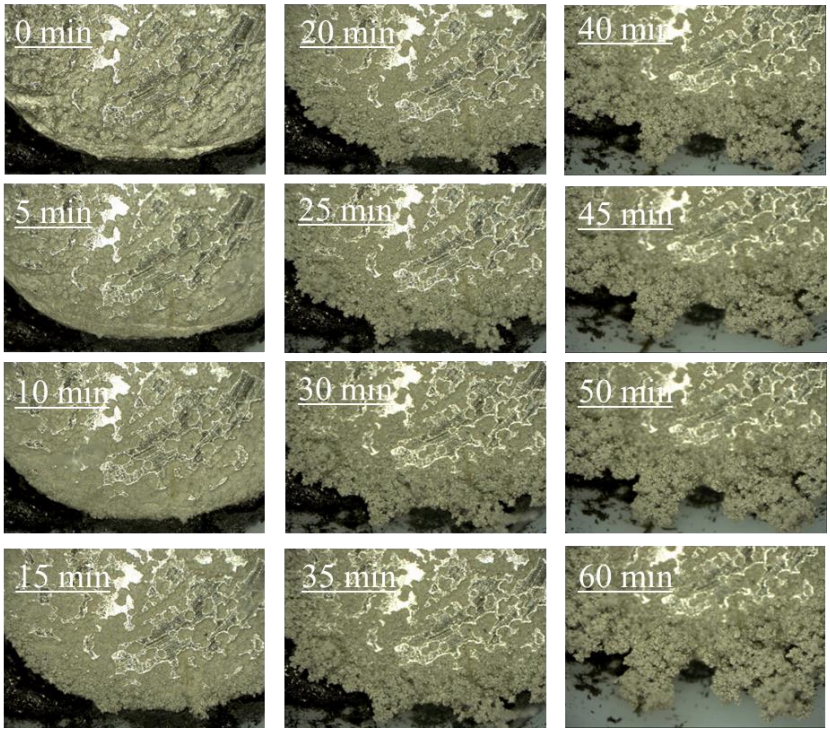

Figure S-2, Baseline electrolyte of LiClO4

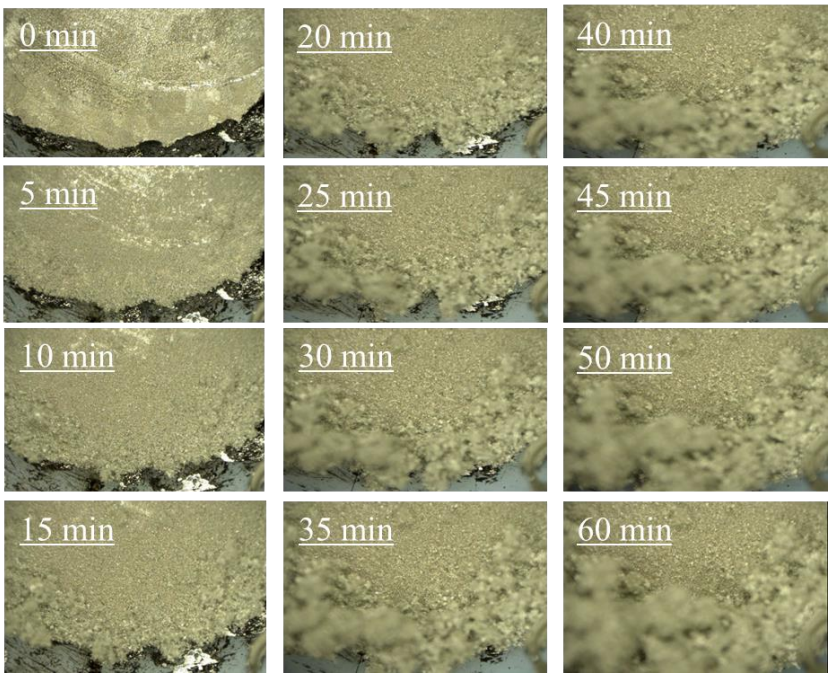

Figure S-3, Baseline electrolyte of LiDFOB

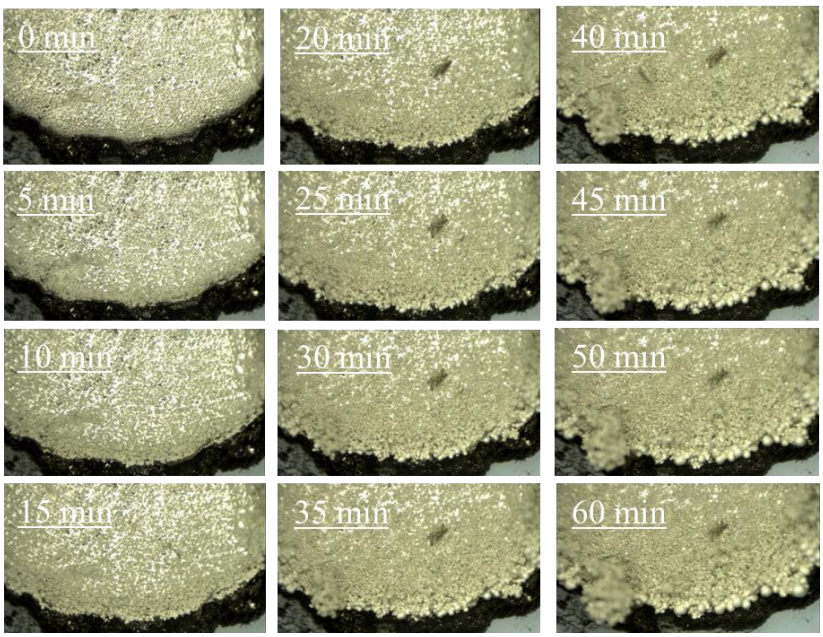

Figure S-4, Baseline electrolyte of LiTFS

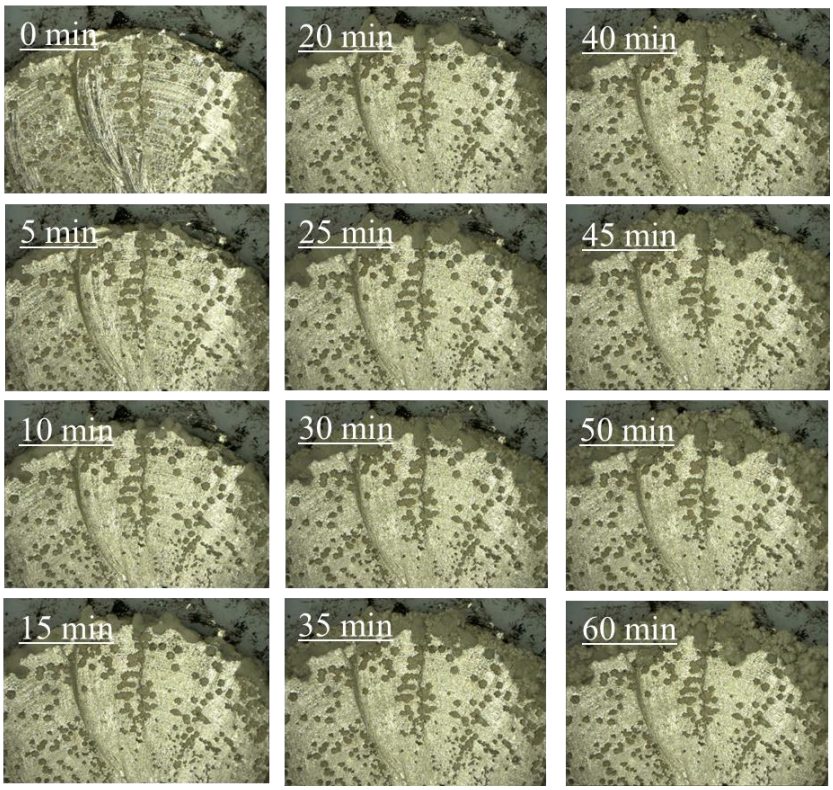

Figure S-5, Baseline electrolyte of LiTFSi

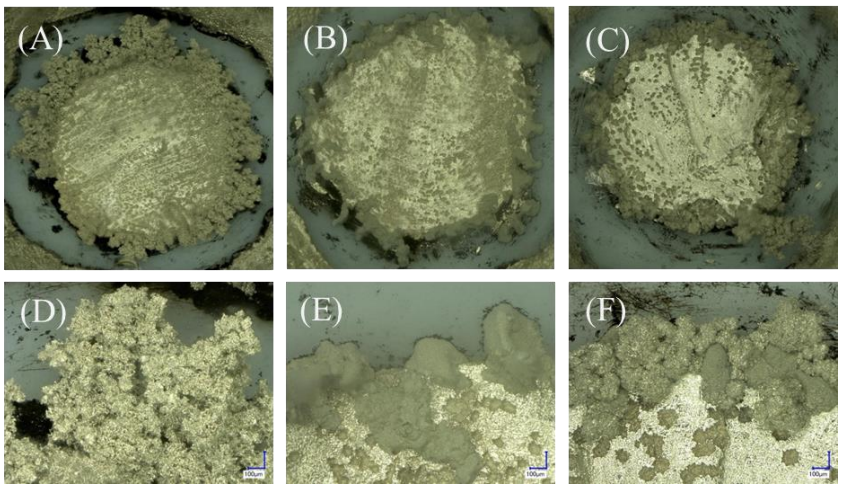

Figure S-6, Baseline electrolyte of LiTFSi in pure DOL (A), in pure DME (B), and in DME/DOL (1:1) mixture (C).

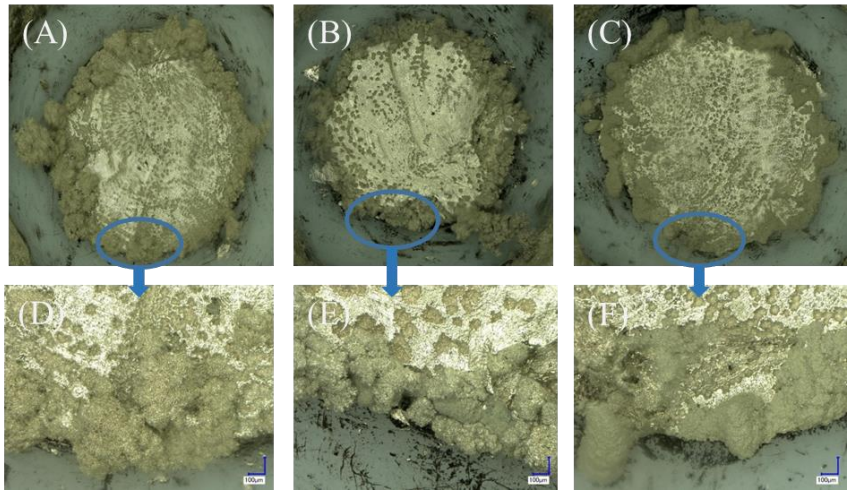

Figure S-7, The optical photographs of lithium electrodes at same electrochemical deposition condition (2 mA, 1hour) in the electrolytes with different concentration of same lithium salt. (A) in 0.5 M LiTFSi/DME/DOL with 0.1 M $LiNO_3$, stitched image, with 100X magnification;(B) in 1.0 M LiTFSi/DME/DOL with 0.1 M $LiNO_3$, stitched image, with 100X magnification; (C) in 2.0 M LiTFSi/DME/DOL with 0.1 M $LiNO_3$, stitched image, with 100X magnification; (D) zoom-in image of (A), with 200X magnification; (E) zoom-in image of (B), with 200X magnification; (F) zoom-in image of (C), with 200X magnification.

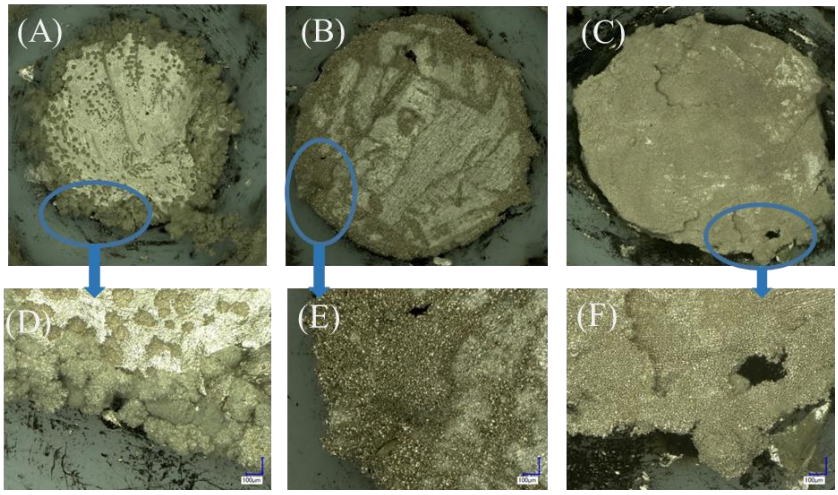

Figure S-8. The optical photographs of lithium electrodes at different electrochemical deposition condition in the same electrolyte (1 M LiTFSi/DME/DOL with 0.1 M $LiNO_3$). (A) 2 mA deposition current for 1 hour, stitched image, with 100X magnification;(B) 0.8 mA deposition current for 2.5 hours, stitched image, with 100X magnification; (C) 0.1 mA deposition current for 20 hour, stitched image, with 100X magnification; (D) zoom-in image of (A), with 200X magnification; (E) zoom-in image of (B), with 200X magnification; (F) zoom-in image of (C), with 200X magnification.

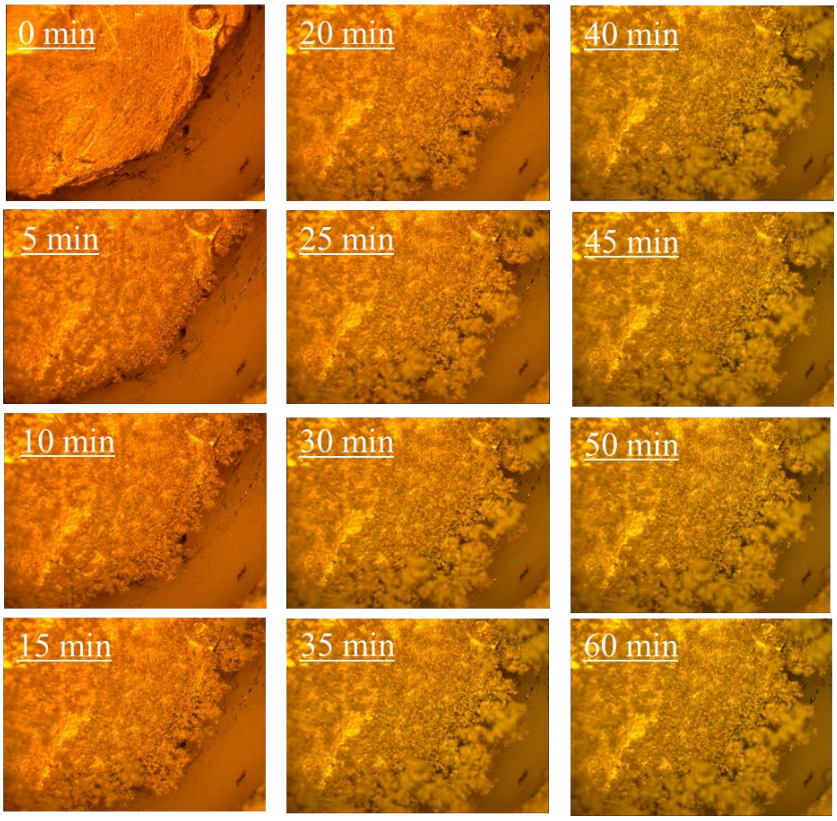

Figure S-9, Electrolyte of LiBETFSi with PS.

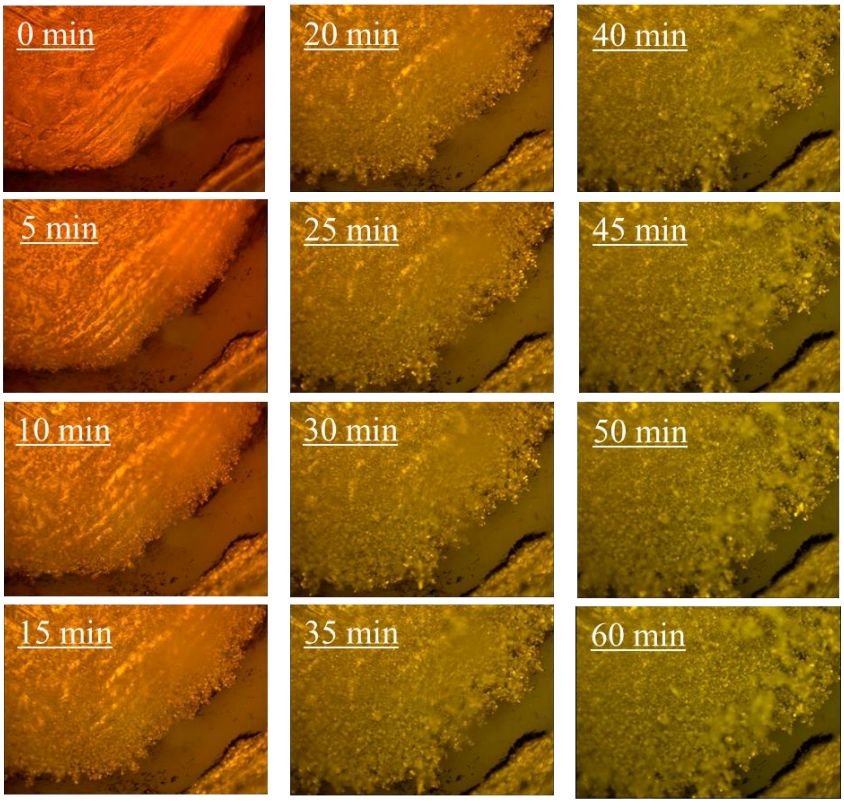

Figure S-10, Electrolyte of LiClO4 with PS.

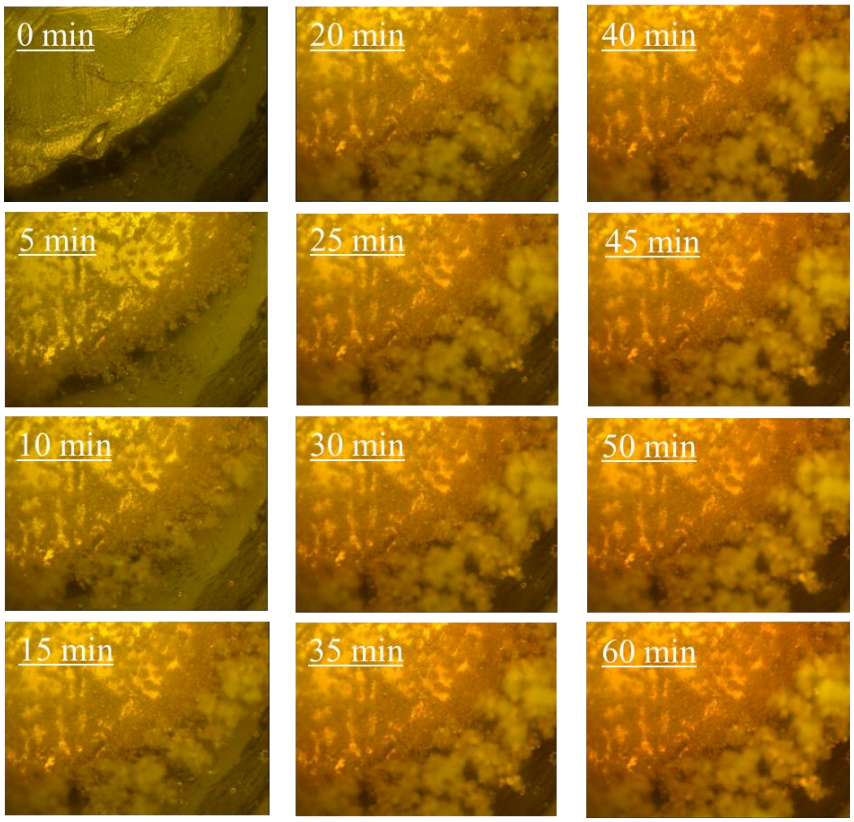

Figure S-11, Electrolyte of LiDFOB with PS.

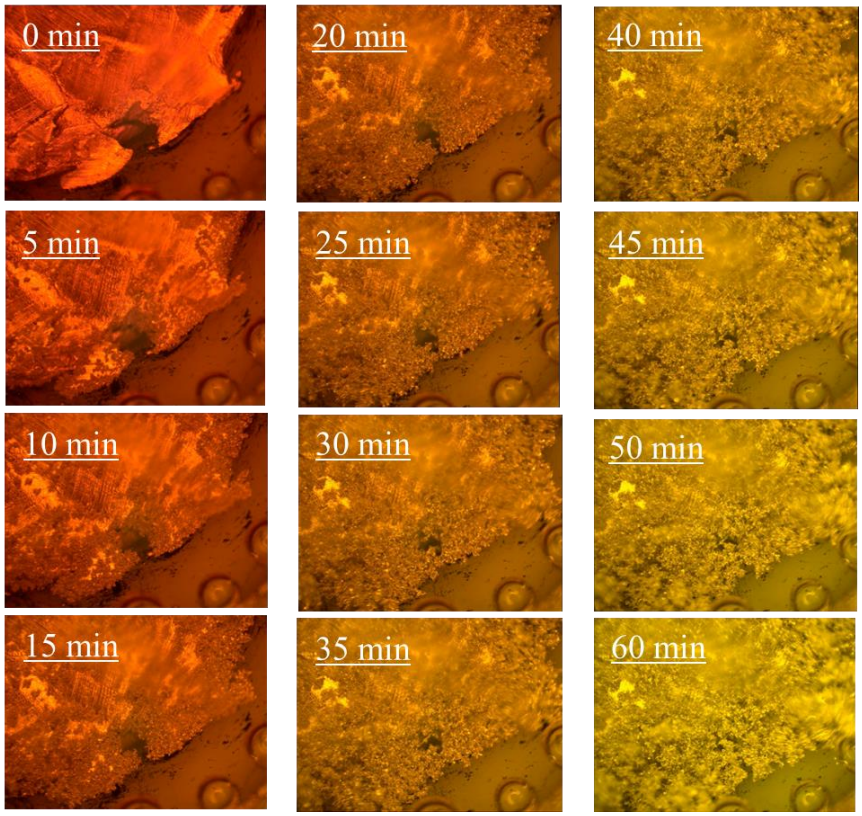

Figure S-12, Electrolyte of LiTFS with PS.

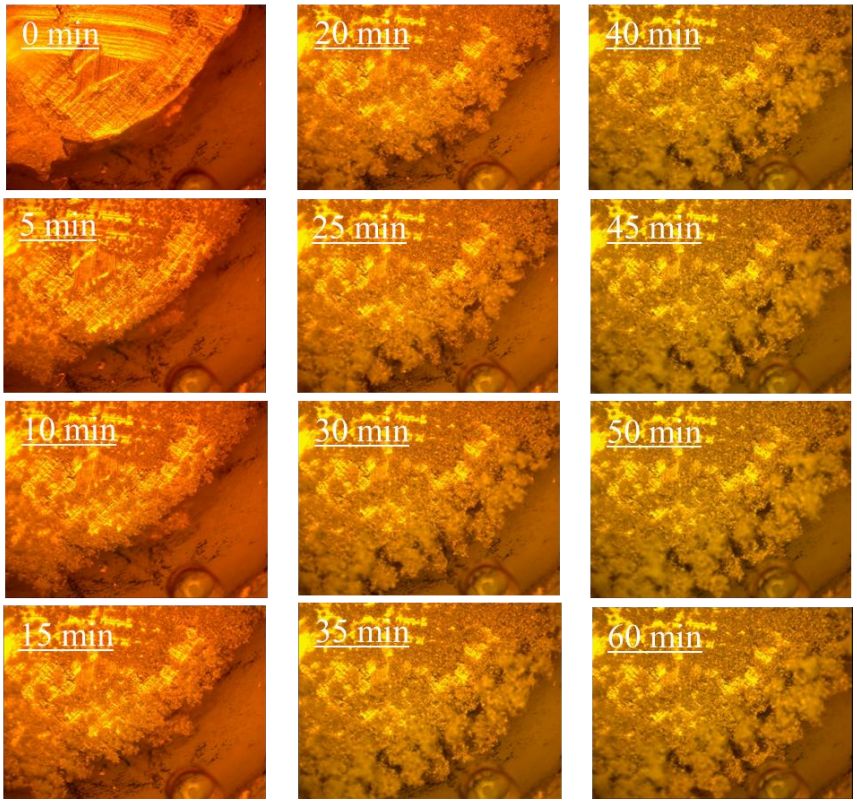

Figure S-13, Electrolyte of LiTFSi with PS.

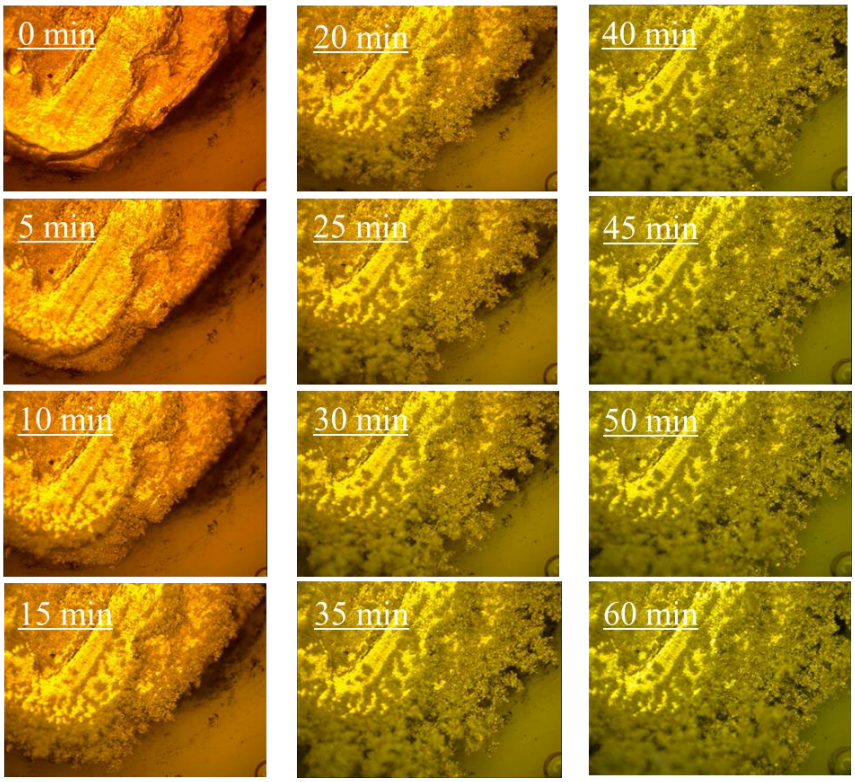

Figure S-14, Electrolyte of LiTFSi with PS and Cs.

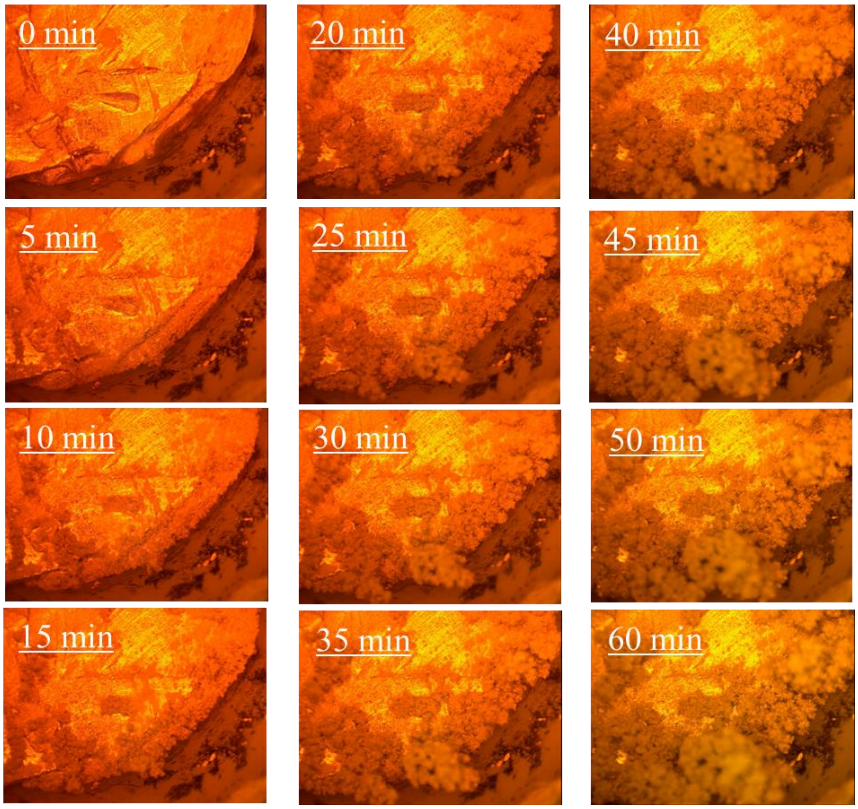

Figure S-15, Electrolyte of LiTFSi with PS and Cs, electrode coated withTEOS.

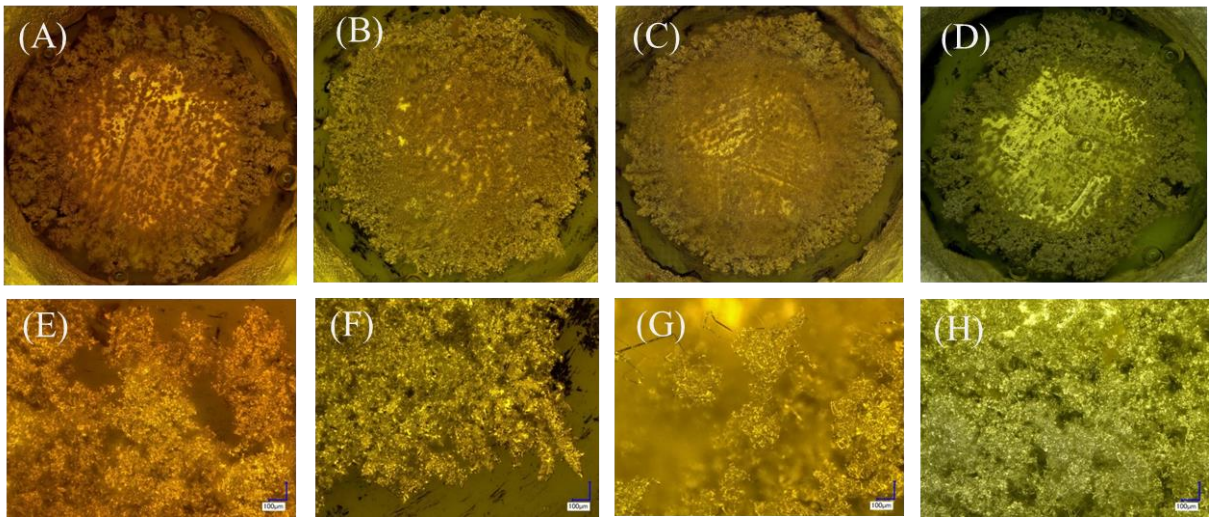

Figure S-16, Electrolytes with PS and Cs,

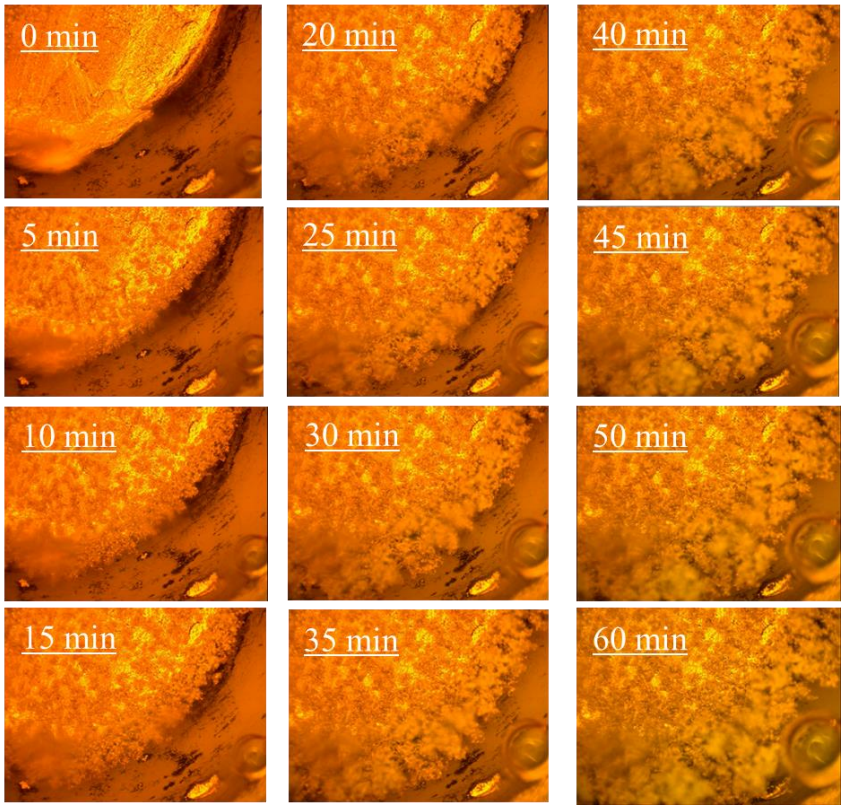

Figure S-17, LiBETFSi electrolytes with PS and Cs,

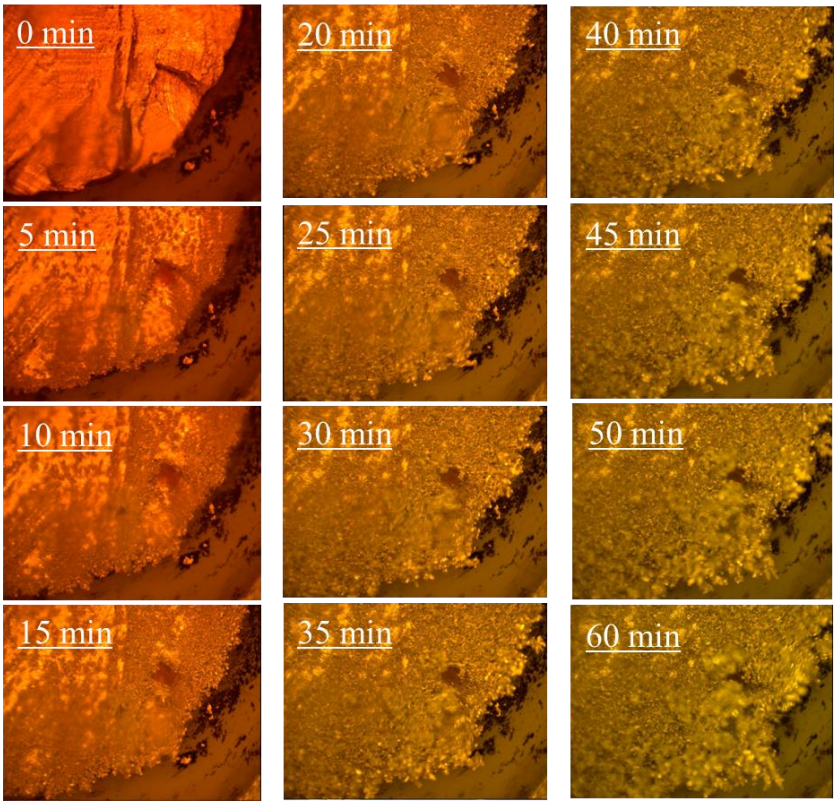

Figure S-18, LiClO4 electrolytes with PS and Cs,

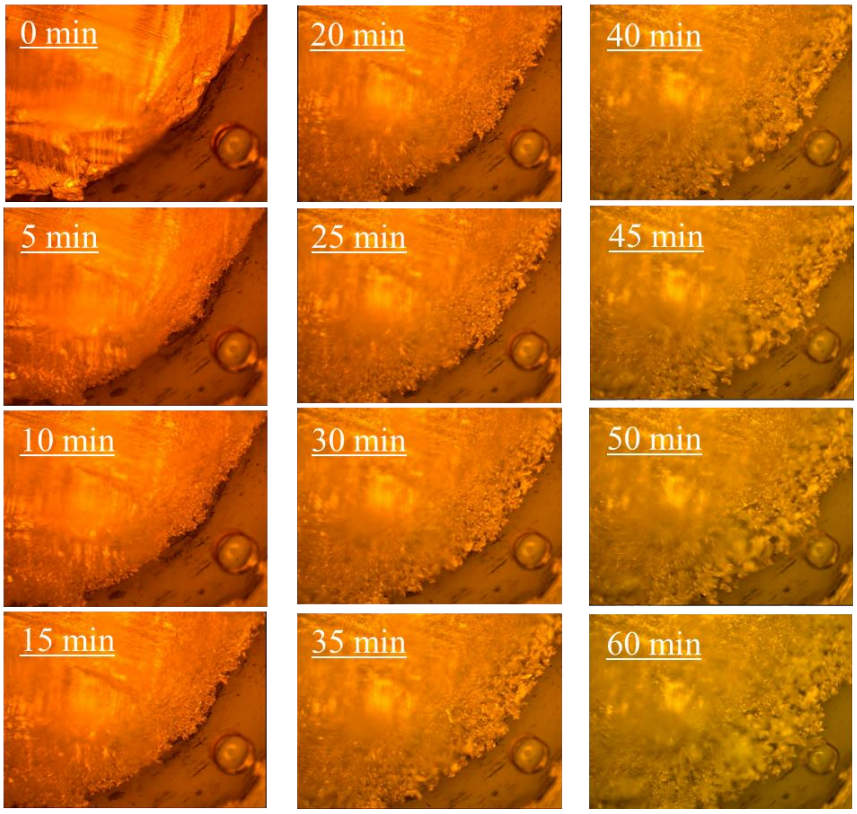

Figure S-19, LiTFS electrolytes with PS and Cs.

6. Bibliography

1. Wu Xu, Jiulin Wang, Fei Ding, Xilin Chen, Eduard Nasybulin, Yaohui Zhang, Ji-Guang Zhang. Lithium Metal Anodes for Rechargeable Batteries. *Energy Environ. Sci.*, 2014, 7, 513-537.
2. Kang Xu. Nonaqueous Liquid Electrolytes for Lithium-Based Rechargeable Batteries. *Chem. Rev.*, 2004, 104, 4303-4417.
3. Isamu Yoshimatsu, Toshiro Hirai, Jun-ichi Yamaki. Lithium Electrode Morphology during Cycling in Lithium Cells. *J. Electrochem. Soc.*, 1988, 135, 2422-2427.
4. Doron Aurbach, Yosef Gpfer, Jacob Langzam. The Correlation between Surface Chemistry, Surface Morphology, and Cycling Efficiency of Lithium Electrodes in a few Polar Aprotic Systems. *J. Electrochem. Soc.*, 1989, 136, 3198-3205.
5. Kiyoshi Kanamura, Soshi Shiraishi, Hiroshi Tamura, Zen-ichiro Takehara. X-Ray Photoelectron Spectroscopic Analysis and Scanning Electron Microscopic Observation of the Lithium Surface Immersed in Nonaqueous Solvents. *J. Electrochem. Soc.*, 1994, 141, 2379-2385.
6. Doron Aurbach, Orit Youngman, Yosef Gpfer, Arie Meitav. The Electrochemical Behavior of 1,3 – Dioxolane – $LiClO_4$ Solutions – I. Uncontaminated Solutions. *Electrochim. Acta*, 1990, 35, 625-638.
7. Doron Aurbach, Orit Youngman, Pnina Dan. The Electrochemical Behavior of 1,3 – Dioxolane – $LiClO_4$ Solutions – II. Contaminated Solutions. *Electrochim. Acta*, 1990, 35, 639-655.
8. Doron Aurbach, I. Weissman, A. Zaban, Orit Chusid (Youngman). Correlation between Surface Chemistry, Morphology, Cycling Efficiency and Interfacial Properties of Li

Electrodes in Solutions Containing Different Li Salts. *Electrochim. Acta*, 1994, 39, 51-71.

9. Soshi Shiraishi, Kiyoshi Kanamura, Zen-ichiro Takehara. Study of the Surface Composition of Highly Smooth Lithium Deposited in Various Carbonate Electrolytes Containing HF. *Langmuir*, 1997, 13, 3542-3549.
10. F. Orsini, A. du Pasquier, B. Beaudoin, J.M. Tarascon, M. Trentin, N. Langenhuizen, E. de Beer, P. Notten. In Situ Scanning Electron Microscopy (SEM) Observation of Interfaces within Plastic Lithium Batteries. *J. Power Sources*, 1998, 76, 19-29.
11. F. Orsini, A. du Pasquier, B. Beaudoin, J.M. Tarascon, M. Trentin, N. Langenhuizen, E. de Beer, P. Notten. In Situ SEM Study of Interfaces in Plastic Lithium Batteries. *J. Power Sources*, 1999, 81-82, 918-921.
12. Katsuhiko Naoi, Mitsuhiro Mori, Yoshinori Naruoka, William M. Lamanna, Radoslav Atanasoski. The Surface Film Formed on a Lithium Metal Electrode in a New Imide Electrolyte, Lithium Bis(perfluoroethylsulfonylimide) [$LiN(C_2F_5SO_2)_2$]. *J. Electrochem. Soc.*, 1999, 146, 462-469.
13. Soshi Shiraishi, Kiyoshi Kanamura, Zen-ichiro Takehara. Surface Condition Changes in Lithium Metal Deposited in Nonaqueous Electrolyte Containing HF by Dissolution-Deposition Cycles. *J. Electrochem. Soc.*, 1999, 146, 1633-1639.
14. Hitoshi Ota, Xianming Wang, Eiki Yasukawa. Characterization of Lithium Electrode in Lithium Imides/Ethylene Carbonate, and Cyclic Ether Electrolytes I. Surface Morphology and Lithium Cycling Efficiency. *J. Electrochem. Soc.*, 2004, 151, A427-A436.

15. L. Gireaud, S. Grugeon, S. Laruelle, B. Yrieix, J.-M. Tarascon. Lithium Metal Stripping/Plating mechanisms Studies: A Metallurgical Approach. *Electrochem. Comm.,* 2006, 8, 1639-1649.

16. Carmen M. Lopez, John T. Vaughey, Dennis W. Dees. Morphological Transitions on Lithium Metal Anodes. *J. Electrochem. Soc.,* 2009, 156, A726-A729.

17. Yuriy V. Mikhaylik, Igor Kovalev, Riley Schock, Karthikeyan Kumaresan, Jason Xu, John Affinito. High Energy Rechargeable Li-S Cells for EV Application. Status, Remaining Problems and Solutions. *ECS Trans.,* 2010, 25, 23-34.

18. Johanna K. Stark, Yi Ding, Paul A. Kohl. Dendrite-Free Electrodeposition and Reoxidation of Lithium-Sodium Alloy for Metal-Anode Battery. *J. Electrochem. Soc.,* 2011, 158, A1100-A1105.

19. Shizhao Xiong, Xie Kai, Xiaobin Hong, Yan Diao. Effecf of LiBOB as Additive on Electrochemical Properties of Lithium-Sulfur Batteries. *Ionics,* 2012,18, 249-254.

20. Wenjun Li, Hao Zheng, Geng Chu, Fei Luo, Jieyun Zheng, Dongdong Xiao, Xing Li, Lin Gu, Hong Li, Xianlong Wei, Qing Chen, Liquan Chen. Effect of Electrochemical Dissolution and Deposition Order on Lithium Dendrite Formation: a Top View Investigation. *Farad. Discuss.,* 2014, 176, 109-124.

21. Masayasu Arakawa, Shi-ichi Tobishima, Yasue Nemoto, Masahiro Ichimura, Jun-ichi Yamaki. Lithium Electrode Cycleability and Morphology Dependence on Current Density. *J. Power Sources,* 1993, 43-44, 27-35.

22. Tetsuya Osaka, Takayuki Homma, Toshiyuki Momma, Hideki Yarimizu. In Situ Observation of Lithium Deposition Processes in Solid Polymer and Gel Electrolytes. *J. Electroanal. Chem.,* 1997, 421, 153-156.

23. C. Brissot, M. Rosso, J.-N. Chazalviel, P. Baudry, S. Lascaud. In Situ Study of Dendrite Growth in Lithium/PEO-Salt/Lithium Cells. *Electrochim. Acta*, 1998, 43, 1569-1574.

24. C. Brissot, M. Rosso, J.-N. Chazalviel, S. Lascaud. Dendritic Growth Mechanisms in Lithium/Polymer Cells. *J. Power Sources*, 1999, 81-82, 925-929.

25. Patrick C. Howlett, Douglas R. MacFarlane, Anthony F. Hollenkamp. High Lithium Metal Cycling Efficiency in a Room-Temperature Ionic Liquid. Electrochem. *Solid State Lett.*, 2004, 7, A97-A101.

26. George H. Lane, Adam S. Best, Douglas R. MacFarlane, Maria Forsyth, Anthony F. Hollenkamp. On the Role of Cyclic Unsaturated Additives on the Behaviour of Lithium Metal Electrodes in Ionic Liquid Electrolytes. *Electrochim. Acta*, 2010, 55, 2210-2215.

27. Kei Nishikawa, Takeshi Mori, Tetsuo Nishida, Yasuhiro Fukunaka, Michel Rosso, Takayuki Homma. In Situ Observation of Dendrite Growth of Electrodeposited Li Metal. *J. Electrochem. Soc.*, 2010, 157, A1212-A1217.

28. H. Sano, H. Sakaebe, H. Matsumoto. Observation of Electrodeposited Lithium by Optical Microscope in Room Temperature Ionic Liquid-based Electrolyte. *J. Power Sources*, 2011, 196, 6663-6669.

29. Tetsuo Nishida, Kei Nishikawa, M. Rosso, Yasuhiro Fukunaka. Optical Observation of Li Dendrite Growth in Ionic Liquid. *Electrochim. Acta*, 2013, 100, 333-341.

30. Jens Steiger, Dominik Kramer, Reiner Monig. Mechanisms of Dendritic Growth Investigated by In Situ Light Microscopy during Electrodeposition and Dissolution of Lithium. *J. Power Sources*, 2014, 261, 112-119.

31. Corey T. Love, Olga A. Baturina, Karen E. Swider-Lyons. Observation of Lithium Dendrites at Ambient Temperature and Below. *ECS Electrochem. Lett.*, 2015, 4, A24-A27.

32. Weiyang Li, Hongbin Yao, Kai Yan, Guangyuan Zheng, Zheng Liang, Yet-Ming Chiang, Yi Cui. The Synergetic Effect of Lithium Polysulfide and Lithium Nitrate to Prevent Lithium Dendrite Growth. *Nat. Commun.*, 2015, 6:7436 doi:10.1038/ncomms8436

33. Dong Zheng, Xiao-Qing Yang, Deyang Qu. Reaction between Lithium Anode and Polysulfide Ions in a Lithium-Sulfur Battery. *ChemSusChem*, 2016, 9, 2348-2350.

34. Grant A. Umeda, Erik Menke, Monique Richard, Kimber L. Stamm, Fred Wudl, Bruce Dunn. Protection of Lithium Metal Surfaces Using Tetraethoxysilane. *J. Mater. Chem.*, 2011, 21, 1593-1599.

35. Peter Paul R. M. L. Harks, Carla B. Robledo, Tomas W. Verhallen, Peter H. L. Notten, Fokko M. Mulder. The Significance of Elemental Sulfur Dissolution in Liquid Electrolyte Lithium Sulfur Batteries. *Adv. Energy Mater.*, 2016, DOI: 10.1002/aenm.201601635.

36. Sheng Shui Zhang. Liquid Electrolyte Lithium/Sulfur Battery: Fundamental Chemsitry, Problems, and Solutions. *J. Power Sources*, 2013, 231, 153-162.

37. Dong Zheng, Dan Liu, Joshua B. Harris, Tianyao Ding, Jingyu Si, Sergei Andrew, Deyu Qu, Xiao-Qing Yang, Deyang Qu. Investigation of the Li-S Battery Mechanism by Real-Time Monitoring of the Changes of Sulfur and Polysulfide Species during the Discharge and Charge. *ACS Appl. Mater. Interfaces*, 2016, DOI:10.1021/acsami.6b08904.

38. Min Sik Park, Sang Bak Ma, Dong Joon Lee, Dongmin Im, Seok-Gwang Doo, Osamu Yamamoto. A Highly Reversible Lithium Metal Anode. *Sci. Rep.*, 2014, 4, 3815.

39. P.S. Rudman, P.A. Flinn, B.L. Averbach. Measurements of Clustering in Solid Al-Zn Alloys. *J. Appl. Phys.*, 1953, 24, 365-366.

40. M. Sobiech, M. Wohlschlogel, U. Welzel, E.J. Mittemeijer, W. Hugel, A. Seekamp, W. Liu, G.E. Ice. Local, Submicron, Strain Gradients as the Cause of Sn Whisker Growth. *J. Appl. Phys.Lett.*, 2009, 94, 221901.

41. Soon-Ki Jeong, Hee-Young Seo, Dong-Hak Kim, Hyun-Kak Han, Jin-Gul Kim, Yoon Bae Lee, Yasutoshi Iriyama, Takeshi Abe, Zempachi Ogumi. Suppression of Dendritic Lithium Formation by Using Concentrated Electrolyte Solutions. *Electrochem. Comm.*, 2008, 10, 635-638.

42. Fei Ding, Wu Xu, Gordon L. Graff, Jian Zhang, Maria L. Sushko, Xilin Chen, Yuyan Shao, Mark H. Engelhard, Zimin Nie, Jie Xiao, Xingjiang Liu, Peter V. Sushko, Jun Liu, Ji-Gang Zhang. Dendrite-Free Lithium Deposition via Self-Healing Electrostatic Shield Mechanism. *J. Am. Chem. Soc.*, 2013, 135, 4450-4456.

43. Joo-Seong Kim, Tae Hoon Hwang, Byung Gon Kim, Jaeyun Min, Jang Wook Choi. A Lithium-Sulfur Battery with a High Areal Energy Density. *Adv. Funct. Mater.*, 2014, 24, 5359-5367.

44. M. Hagen, S. Dorfler, P. Fanz, T. Berger, R. Speck, J. Tubke, H. Althues, M.J. Hoffmann, C. Scherr, S. Kaskel. Development and Costs Calculation of Lithium-Sulfur Cells with High Sulfur Load and Binder Free Electrodes. *J. Power Sources*, 2013, 224, 260-268.

45. Ning Ding, Sheau Wei Chien, T.S. Andy Hor, Zhaolin Liu, Yun Zong. Key Parameters in Design of Lithium-Sulfur Batteries. *J. Power Sources*, 2014, 269, 111-116.

46. Dongping Lv, Jianming Zheng, Qiuyan Li, Seth Ferrara, Zimin Nie, Layla B. Mehdi, Nigel D. Browning, Ji-Guang Zhang, Gordon L. Graff, Jun Liu, Jie Xiao. High Energy Density Lithium-Sulfur Batteries: Challenges of Thick Sulfur Cathodes. *Adv. Energy Mater.*, 2015, 5, 1402290.
47. Xiwen Wang, Tao Gao, Fudong Han, Zhaohui Ma, Zhian Zhang, Jie Li, Chunsheng Wang. Stabilizing High Sulfur Loading Li-S Batteries by Chemisorption of Polysulfide on Three-Dimensional Current Collector. *Nano Energy*, 2016, DOI:10.1016/j.nanoen.2016.10.049.
48. Zhe Yuan, Hong-Jie Peng, Jia-Qi Huang, Xin-Yan Liu, Dai-Wei Wang, Xin-Bing Cheng, Qiang Zhang. Hierarchical Free-Standing Carbon-Nanotube Paper Electrode with Ultrahigh Sulfur-Loading for Lithium-Sulfur Batteries. *Adv. Funct. Mater.*, 2014, 24, 6105-6112.
49. Long Qie, Arumugam Manthiram. High-Energy-Density Lithium-Sulfur Batteries Based on Blade-Cast Pure Sulfur Electrodes. *ACS Energy Lette.*, 2016, 1, 46-51.
50. Sheng-Heng Chung, Chi-Hao Chang, Arumugam Manthiram. A Carbon-Cotton Cathode with Ultrahigh-Loading Capability for Statically and Dynamically Stable Lithium-Sulfur Batteries. ACS Nano, 2016, 10, 10462-10470.
51. Herbert D, Ulam J. Electric dry cells and storage batteries. US Pat. ,3043896(1962)
52. Xiulei Ji, Kyu Tae Lee, and Linda F. Nazar. (17 May 2009)"A highly ordered nanostructured carbon-sulphur cathode for lithium-sulphur batteries." Nature Materials
53. She, Z. W.; Sun, Y. M.; Zhang, Q. F.; Cui, Y. Chem. Soc. Rev. 2016, 45, 5605–5634.